AD-A064 704 HARVARD UNIV CAMBRIDGE MA DIV OF APPLIED SCIENCES F/G 20/13
HOLE STATISTICS IN DENSE RANDOM PACKING.(U)
DEC 78 H J FROST N00014-77-C-0002
UNCLASSIFIED TR-6 NL

1 OF 1
AD A064704

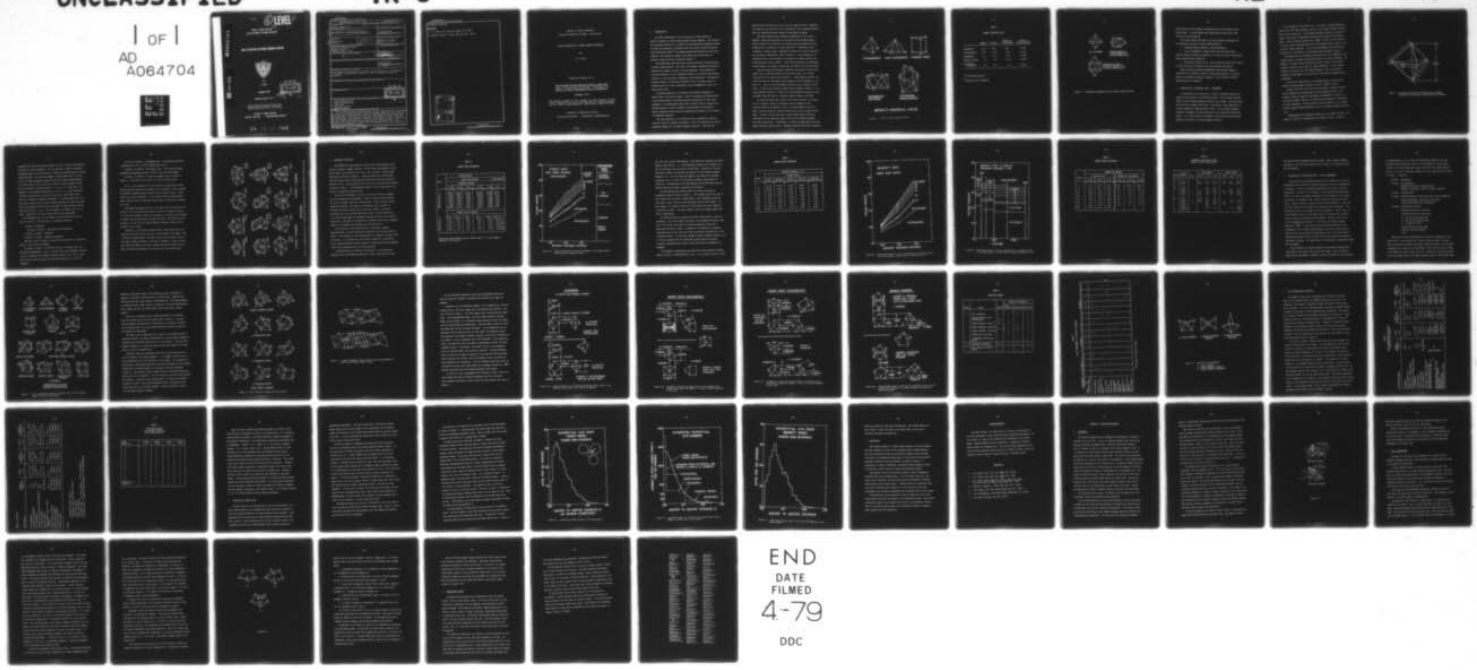

END
DATE FILMED
4-79
DDC

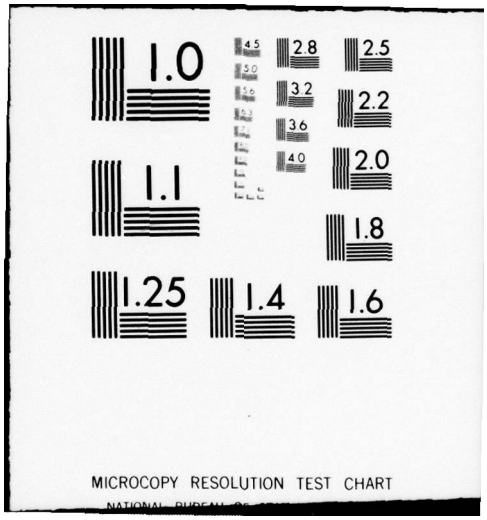
1.0
1.1
1.25
1.4
1.6
1.8
2.0
2.2
2.5
2.8
3.2
3.6
4.0
4.5
5.0
MICROCOPY RESOLUTION TEST CHART

(6) LEVEL II

Office of Naval Research

Contract N00014 77-C-0002 NR-039-136

HOLE STATISTICS IN DENSE RANDOM PACKING

By

H. Frost

December 1978

Technical Report No. 6

Division of Applied Sciences

Harvard University Cambridge, Massachusetts

Unclassified

SECURITY CLASSIFICATION OF THIS PAGE (When Data Entered)

REPORT DOCUMENTATION PAGE	READ INSTRUCTIONS BEFORE COMPLETING FORM
1. REPORT NUMBER: Technical Report No. 6	2. GOVT ACCESSION NO. / 3. RECIPIENT'S CATALOG NUMBER
4. TITLE (and Subtitle): HOLE STATISTICS IN DENSE RANDOM PACKING	5. TYPE OF REPORT & PERIOD COVERED: Interim Report
	6. PERFORMING ORG. REPORT NUMBER
7. AUTHOR(s): H.J. Frost (10) (14) TR-6	8. CONTRACT OR GRANT NUMBER(s): N00014-77-C-0002 (15)
9. PERFORMING ORGANIZATION NAME AND ADDRESS: Division of Applied Sciences, Harvard University, Cambridge, Mass. 02138	10. PROGRAM ELEMENT, PROJECT, TASK AREA & WORK UNIT NUMBERS
11. CONTROLLING OFFICE NAME AND ADDRESS: (9) Technical rept.,	12. REPORT DATE: December 1978 (11) / 13. NUMBER OF PAGES: 60 (12) 61p.
14. MONITORING AGENCY NAME & ADDRESS (if different from Controlling Office)	15. SECURITY CLASS. (of this report): Unclassified / 15a. DECLASSIFICATION/DOWNGRADING SCHEDULE

16. DISTRIBUTION STATEMENT (of this Report)

This document has been approved for public release and sale; its distribution is unlimited. Reproduction in whole or in part is permitted by the U.S. Government.

17. DISTRIBUTION STATEMENT (of the abstract entered in Block 20, if different from Report)

DDC RECEIVED FEB 16 1979 B

18. SUPPLEMENTARY NOTES

19. KEY WORDS (Continue on reverse side if necessary and identify by block number)

Dense Random Packing
Bernal Canonical Holes
Deltahedra
Interstitial Sites
Metallic Glasses

20. ABSTRACT (Continue on reverse side if necessary and identify by block number)

The structure of dense random packings of hard spheres has been investigated in terms of the polyhedral holes between the spheres, using both all triangular-faced polyhedra called deltahedra, and local arrangements allowing three- and four-edged faces. Two models were analyzed: The mechanical model of Finney,[1] and the computer-generated model of Bennett.[2] The number and sizes of the sites for small interstitial spheres were also calculated for both models. The structural units described and the results may be applicable to the structure of liquid metals and metallic glasses.

DD FORM 1 JAN 73 1473 EDITION OF 1 NOV 65 IS OBSOLETE
S/N 0102-014-6601

410 457

Unclassified

SECURITY CLASSIFICATION OF THIS PAGE (When Data Entered)

20. Abstract continued

References:

1. J.L. Finney, Proc. Roy. Soc. 319A, 479, (1970).

2. Charles H. Bennett, J. Appl. Phys. 43, 2727, (1972).

Office of Naval Research

Contract N00014-77-C-0002 NR-039-136

HOLE STATISTICS IN DENSE RANDOM PACKINGS

By

H.J. Frost

Technical Report No. 6

December 1978

The research reported in this document was made possible through support extended the Division of Applied Sciences, Harvard University, by the Office of Naval Research, under Contract N00014-77-C-0002.

Division of Applied Sciences

Harvard University · Cambridge, Massachusetts

1. INTRODUCTION

The first approximation to the structure of liquid metals or metallic glasses is a dense random packing of hard spheres. The structure was initially studied by J.D. Bernal[1] who characterized a mechanical model of single-sized spheres, arranged without any regular crystal structure. Other mechanical models[2,3] and computer-generated models[4] have also been studied. The connection between these models and the structure of metallic glasses has been reviewed by Cargill.[5]

Three approaches have been taken toward statistical characterization of dense random packings. The first is by radial distribution functions, measuring the number of pairs at various spacings. This procedure is attractive because it can be compared directly to the radial distribution functions of real materials, measured by x-ray techniques. The method is limited, however, to pairwise correlation, and it can give little information about how often a particular local arrangement of three or more points might occur.

The second approach is to describe the average arrangement of spheres about a particular sphere. Scott[3] introduced this approach with a pole figure showing the average angular distribution of first shell neighbors. This same approach was used by Finney[2] when he reported the characteristics of Voronoi polyhedra (the polyhedron surrounding a sphere, bounded by faces which are perpendicular bisectors of the vectors to neighboring spheres).

The third approach is to characterize the arrangments of spheres around the holes in between the spheres. That is to describe the various polyhedra formed with the sphere centers as corners. This was the

approach used by Bernal and led to his five canonical holes. Recently, this approach was revived by E.J.W. Whittaker,[6] who re-examined Bernal's model and identified several shapes not mentioned by Bernal.

This paper reports a more extensive examination of this third approach, reporting statistics on the various holes between spheres. Bernal reported that almost all the volume could be divided into five canonical holes (allowing for some distortion): Tetrahedron, half-octahedron, trigonal prism, Archimedian antiprism (or square antiprism) and tetragonal dodecahedron, shown in Figure 1. From inspection of a mechanical model of hard spheres, he reported the number percents and volume percents given in Table 1. With the known density, and assuming regular shapes, the number of shapes per 100 spheres can be calculated.

There has been some confusion regarding the shapes of these holes: Bernal used a trigonal prism with three square faces, and a square antiprism with two square faces (Figure 1). These shapes, however, are often pictured with the square faces capped with half-octahedra, as in Figure 2. (They are then deltahedra--polyhedra with triangles for all faces). Bernal also considered separate half-octahedra (Figure 1), not full octahedra (Figure 2). Some of his half-octahedra are parts of full octahedra; some are caps for trigonal prisms of square antiprisms.

An important point here is that in the actual packing, the square faces on trigonal prisms or antiprisms could be capped by other trigonal prisms or antiprisms. Thus, a structure based on the five small canonical holes can contain structures that are not simple deltahedra. In fact, we shall see that a dense random packing cannot be described as being completely made up of the five simple deltahedra with small distortions. Furthermore, it cannot be described by the five smaller Bernal canonical holes. Whittaker used the five Bernal canonical

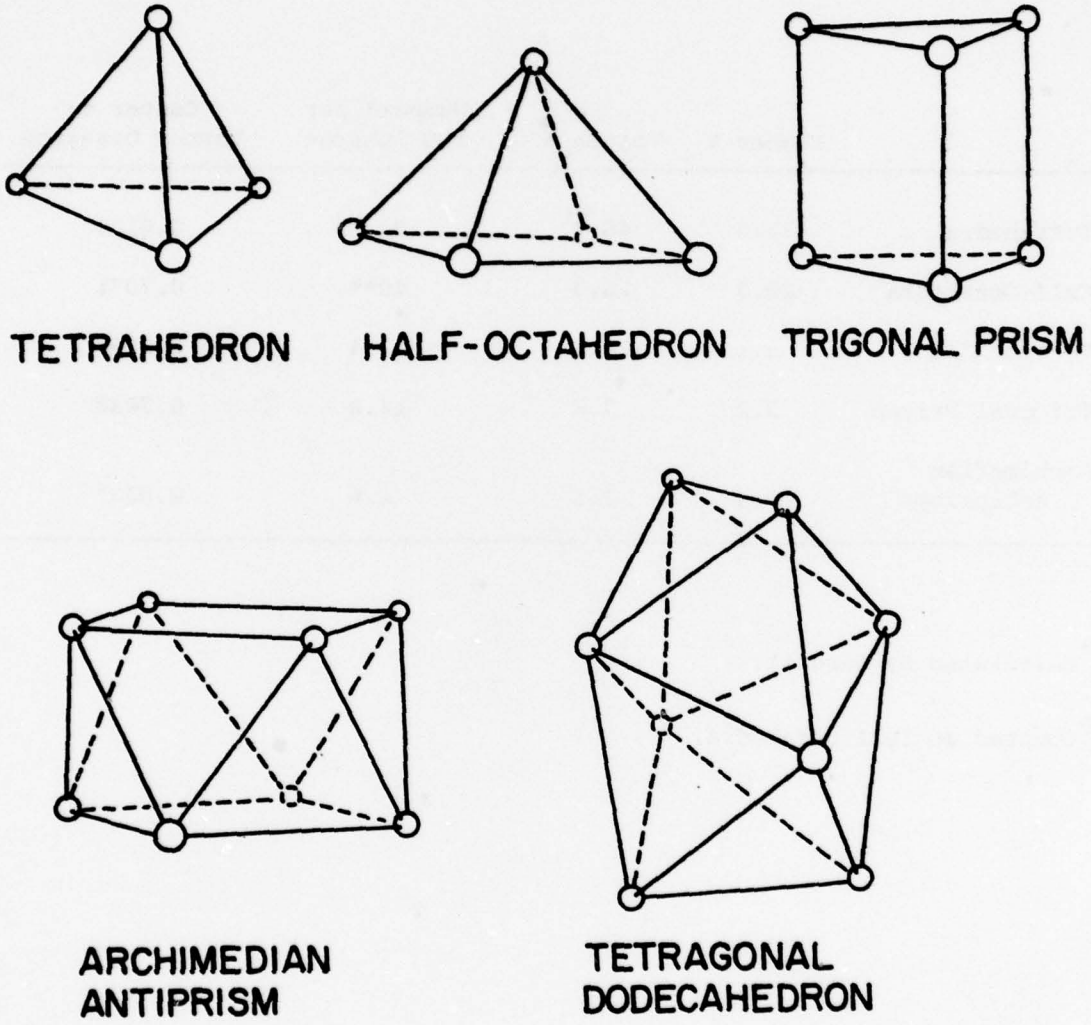

BERNAL'S CANONICAL HOLES

Figure 1. The five Bernal canonical holes.

TABLE 1

BERNAL CANONICAL HOLES

	Number %	Volume %	Number* per 100 Spheres	Center to Vertex Distance
Tetrahedra	73.0	48.4	292	0.6124
Half-Octahedra	20.3	26.9	40**	0.7071
Dodecahedra	3.1	14.8	12.4	0.6766
Trigonal Prisms	3.2	7.8	12.8	0.7638
Archimedian Antiprisms	0.4	2.1	1.6	0.8227

*Calculated by Cargill.

**Counted as full octahedra.

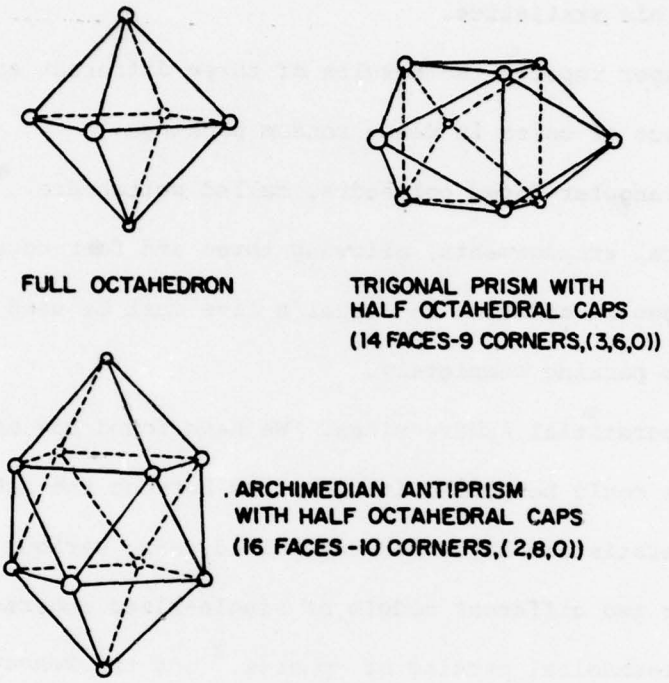

Figure 2. Deltahedra generated from the Bernal canonical holes.

holes plus four other shapes to describe most of the cavities in the Bernal model. He also deduced what approximations Bernal must have used to get his statistics.

This paper reports the results of three different approaches to the statistics of holes in dense random packings:

1. Triangular-faced polyhedra, called deltahedra.

2. Local arrangements, allowing three and four-edged faces. Several shapes in addition to Bernal's five must be used to describe the dense random packing completely.

3. Interstitial sphere sites. We have found how many small spheres of what size could be placed in the sites between the spheres.

These statistics have been determined using various computer programs for two different models of single-sized spheres; the Finney model of a mechanical packing of spheres,[2] and the Bennett computer generated array of spheres.[4]

2. DESCRIPTION OF STRUCTURAL UNITS: DELTAHEDRA

A description of the structure in terms of triangular-faced polyhedra can be achieved in the following manner: Any two sphere centers within a chosen nearest-neighbor distance form an edge. Any three edges that join as a triangle form a face. And finally, each volume that is totally enclosed by faces describes a hole. If the nearest-neighbor distance is changed, the hole description of any particular region may change. In a large cluster, the numbers of the various types of holes depend on the choice of nearest-neighbor distance.

If the distance is too small (e.g., less than 1.1 sphere diameters) there will be few faces defined, and only a few volumes enclosed, leaving most of the volume open. If the nearest-neighbor distance is chosen too large, it may lead to ambiguous descriptions of certain local arrangements. Using a distance greater than $\sqrt{12/7} = 1.309307$, the five points in Figure 3 may be described either as two tetrahedra base to base, or as a ring to three tetrahedra. This is the arrangement that allows interpenetration of tetrahedra at the minimum nearest-neighbor distance.

The possibility of interpenetration means that the deltahedra do not always provide a suitable unique description of an array of spheres. For example, the simple cubic structure provides no faces if the nearest-neighbor distance is less than $\sqrt{2}$ sphere diameters. If the neighbor distance is greater than $\sqrt{2}$ sphere diameters, then all cube-face diagonals become edges, and the volume is filled with interpenetrating tetrahedra.

To avoid the complications of interpenetration, we should only consider nearest-neighbor distance less than $\sqrt{12/7} = 1.309307$.

Another difficulty with large nearest-neighbor distances is that certain shapes may be subdivided into less descriptive units. The interior distance through the tetragonal dodecahedron is 1.2892. At any larger neighbor distance, an undistorted dodecahedron is described as seven tetrahedra. We have used one larger distance, 1.30, at which we find slightly fewer dodecahedra than at the smaller neighbor distance 1.28.

Deltahedra may be catalogued according to the number of faces. The number of corners is constrained by the number of faces. Since we

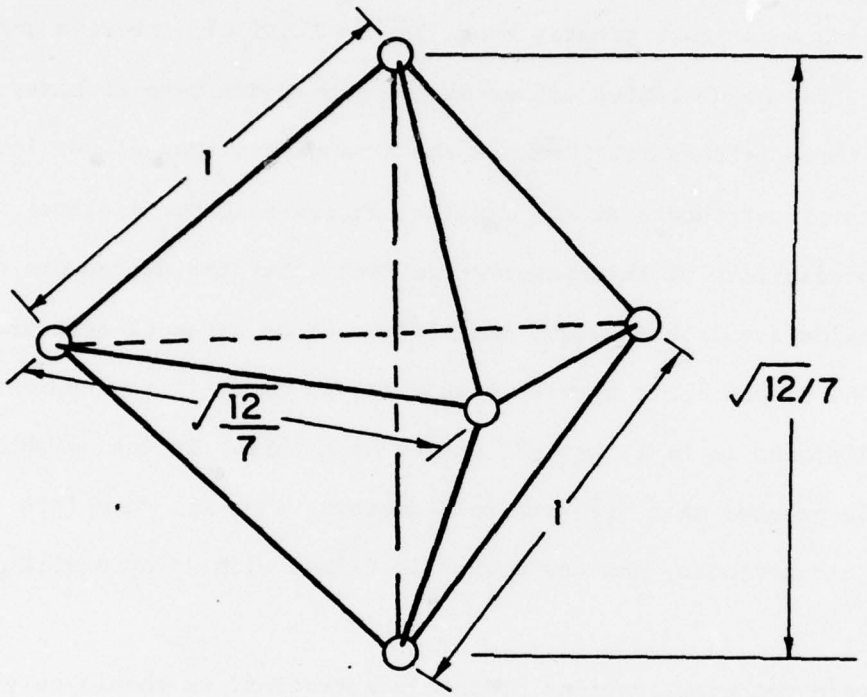

Figure 3. Arrangement showing the minimum nearest neighbor distance that allows for interpenetrating tetrahedra.

consider both convex and concave shapes, our list is longer than previous listings of convex deltahedra. Our list does not include all possible deltahedra shapes, but concentrates on those that actually occur in dense random packings. For any given number of faces larger than 12, there are two or more topological shapes that occur in dense random packings. To identify them, we can use a set of three (or four) integers, which give the number of corners at which 4, 5, or 6 (or 7) faces meet. For examples, the tetragonal dodecahedron is (4,4,0). No large polyhedron can have a convex corner with only three faces, because that corner would be considered a separate tetrahedron. For some shapes with 16 or more faces, certain sets of corner numbers describe more than one shape. These are separately identified by the number of edges between 4-faced and 6-faced corners: N_{6-4}. This is adequate for shapes with 16 or 18 faces. Shapes with 20 or more faces have not been catalogued.

The deltahedra that are not based on Bernal canonical holes are shown in Figure 4. The following is a complete catalogue:

4 Faces - Tetrahedron

(6 Faces, 5 Corners: Described as two Tetrahedra.)

8 Faces, 6 Corners: Octahedron

10 Faces, 7 Corners: Pentagonal Bipyramid.

This was not one of Bernal's canonical holes because it is approximately a ring of five tetrahedra.

12 Faces, 8 Corners: The primary form is a canonical hole, the tetragonal dodecahedron, (4,4,0). Another form, the hexagonal bipyramid, (6,0,2) is possible for neighbor distances greater than $2/\sqrt{3} = 1.1547$. This form was never observed in dense random packings, so it may be neglected.

14 Faces, 9 Corners. Two shapes occur: the trigonal prism with octahedral caps (3,6,0) and an unnamed shape (4,4,1).

16 Faces, 10 Corners: Five shapes occur. The canonical shape, Archimedian antiprism with caps (2,8,0), is not the most common.

18 Faces, 11 Corners: At least six shapes occur, as shown in Figure 4. Other shapes are possible, but have not been found.

For 12 or more corners (20 or more faces) the topological forms become even more numerous, and haven't been catalogued. The structures we analyzed contained numerous holes with more than 20 faces. These holes are not open vacancies: no unit sphere could be placed inside them. They are flat or elongated regions where the packing is slightly more open.

The method described above does not require that all faces and all edges fit into the walls that divide the array into separate volumes. It is entirely possible to have an edge that is not part of any triangle of edges, and therefore does not border any face. Such edges are very unlikely to occur, for the larger neighbor distances, except on the surface of the cluster.

Similarly, it is entirely possible that a particular face is not joined to any other face on one, two, or even three of its edges. This is usually a surface effect, but also occurs in the interior, even at the larger neighbor distances. We found no examples of interior faces with three free edges, but interior faces with one free edge do occur. Such a face must necessarily occur within one of the larger holes.

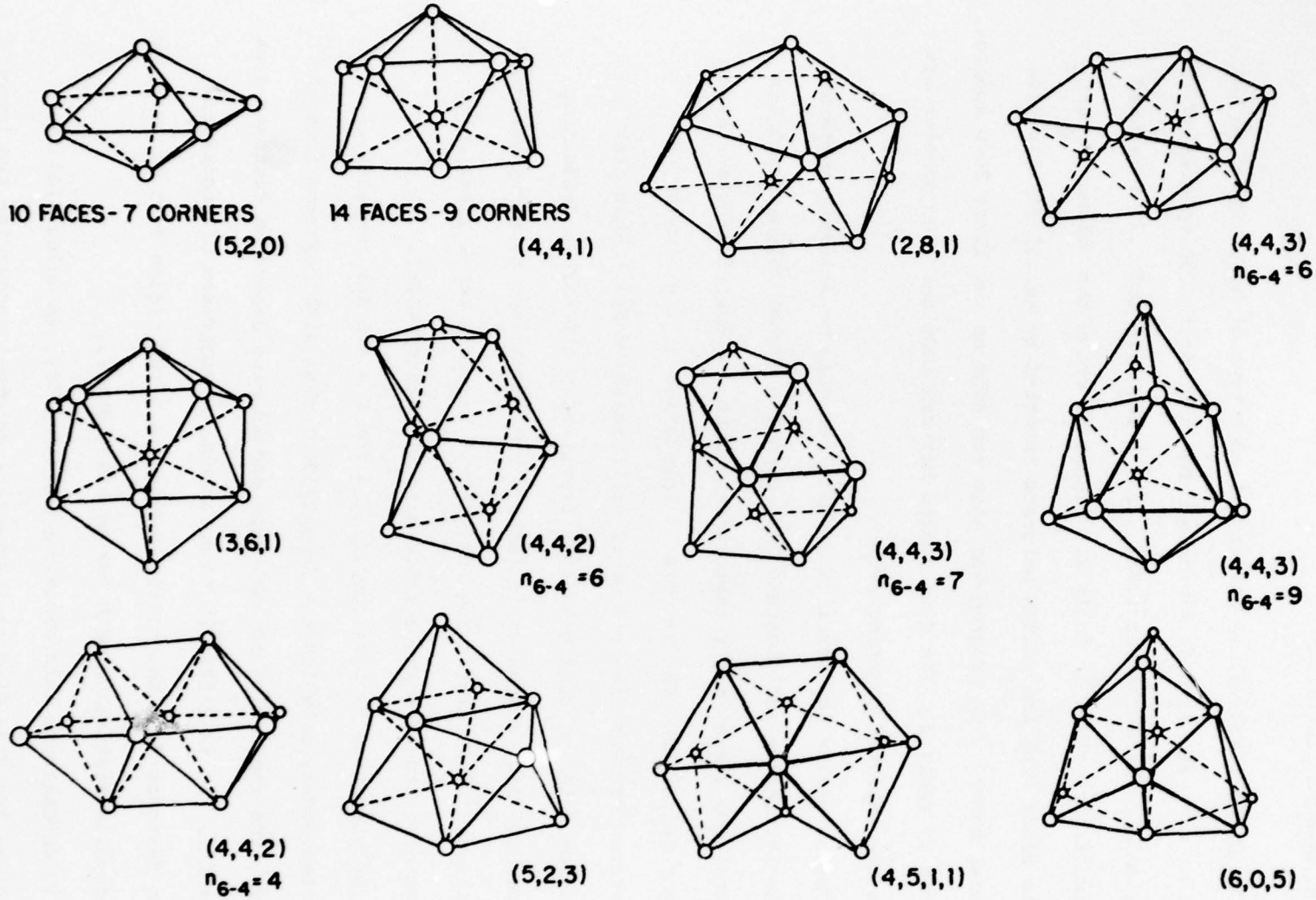

DELTAHEDRA

Figure 4. Deltahedra with up to 11 corners and 18 faces that are not based on Bernal's canonical holes.

3. DELTAHEDRA STATISTICS

The numbers and volume percent of each type of hole depend on the choice of nearest neighbor distance. For the inner 1000 spheres of the Finney model, the distances 1.20, 1.25, 1.26, 1.28 and 1.30 were used. The results are given in Table 2. Figure 5a shows the volume percent results along with the volume percents reported by Bernal for his five canonical holes. The program was also run once on the inner 2000 spheres, as shown in Table 2. The differences between 1000 and 2000 spheres are within the expected counting errors.

These results and Bernal's results can only be directly compared for the tetrahedra and dodecahedra. Bernal's higher volume fractions for these two shapes might have three causes: A more flexible nearest neighbor definition, the effects of boundaries of the cluster, or differences between Finney's model and Bernal's model. Whittaker considered this and concluded that Bernal used a flexible definition that counted some shapes as tetrahedra that would not be so by stricter definitions. Whittaker's own analysis of Bernal's model gives comparable numbers of tetrahedra and octahedra to the Finney model.

The situation is more complicated for the Bennett computer generated model, in which the density decreases with distance from the center. The statistics of hole type should also depend on distance from the center. It is difficult to do an exact comparison of statistics versus distance from the center, because a large region must be examined to get valid statistics with low counting errors.

To demonstrate this variation with density, we calculated the statistics for five different spherical volumes, containing the inner

TABLE 2

FINNEY MODEL DELTAHEDRA

Faces	Volume Percent					
	Inner 1000 Spheres					2000 Spheres
	Neighbor Distance					
	1.20	1.25	1.26	1.28	1.30	1.30
4	19.01	29.08	30.70	35.30	40.30	40.24
8	6.66	11.47	11.91	13.95	15.82	15.77
10	0.29	0.59	0.58	1.04	1.37	1.34
12	5.15	8.08	8.54	9.62	9.48	9.14
14	0.49	2.14	2.71	3.40	3.88	3.75
16	1.21	2.96	3.32	3.65	2.58	3.03
18	1.84	4.35	4.28	3.76	2.47	2.52
20	1.46	3.79	2.72	3.27	3.69	3.48
>20	63.89	37.54	35.25	26.01	20.41	20.73
	Number per 100 Spheres					
4	121.4	182.4	192.0	219.7	249.6	249.5 ± 3.5*
8	10.7	18.2	18.8	21.9	24.7	24.9 ± 1.1
10	0.3	0.7	0.6	1.1	1.5	1.5 ± 0.27
12	4.5	7.0	7.3	8.2	7.9	7.7 ± 0.6
14	0.3	1.4	1.8	2.3	2.5	2.5 ± 0.35
16	0.7	1.7	1.9	2.1	1.4	1.7 ± 0.3
18	0.9	2.1	2.1	1.8	1.2	1.2 ± 0.24
20	0.6	1.6	1.2	1.4	1.6	1.4 ± 0.26

*Errors given are counting errors, $\sqrt{N}/20$, where N is the number of observed in 2000 points.

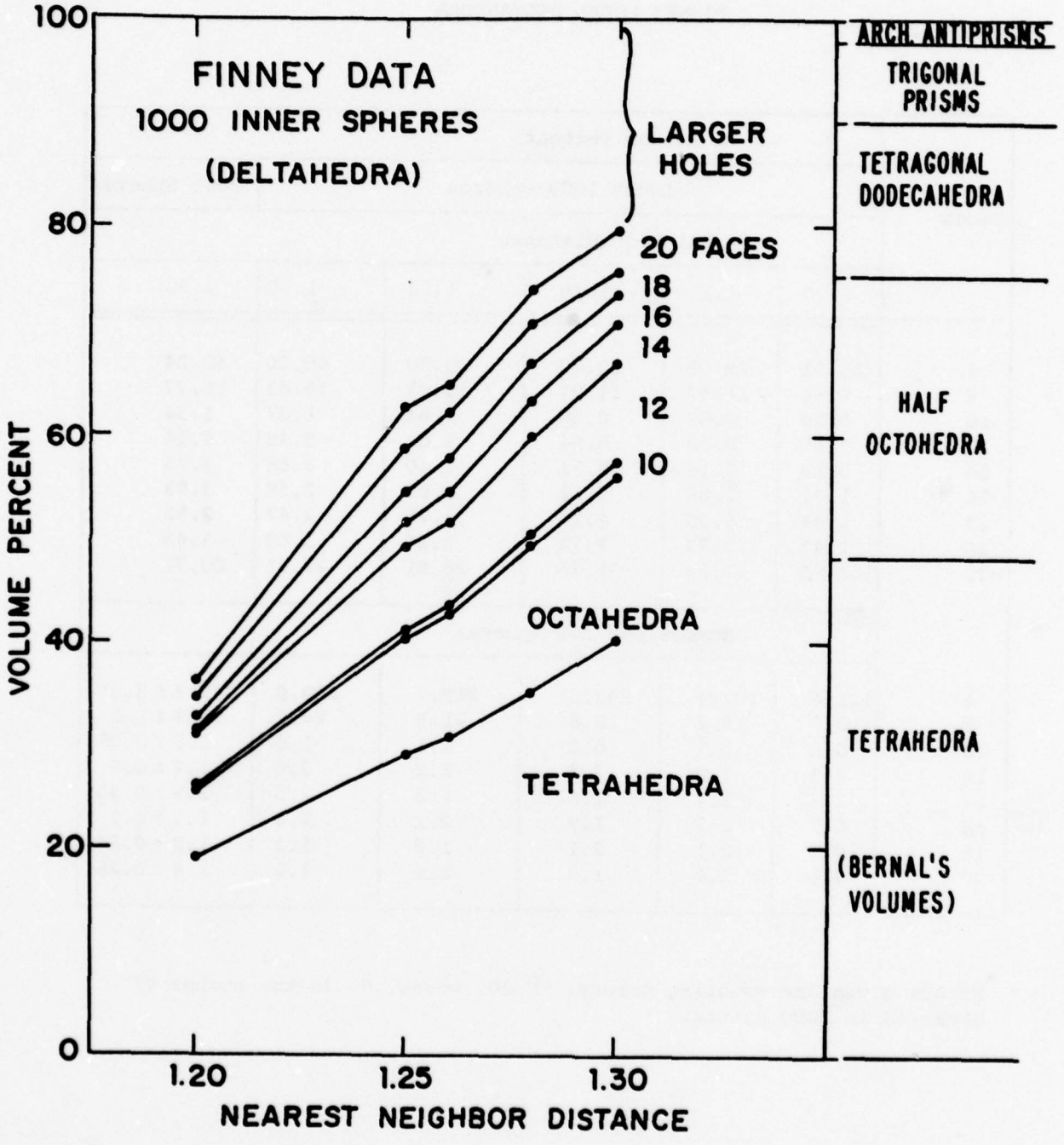

Figure 5a. Volume percentage of various deltahedra in the Finney model, versus nearest neighbor distance.

200, 348, 600, 100 and 1500 spheres. The results are presented as shells between these limits: i.e., the difference between the 200 sphere core and the 348 sphere core gives the 200-348 shell. Results for this are tabulated in Table 3 and plotted in Figure 6 for the nearest neighbor distance 1.30. For the inner 1000 spheres, the results for neighbor distances 1.20, 1.25, and 1.30 are given in Table 4 and plotted in Figure 5b. The reversal of the trend between the 200-348 shell and the 348-600 shell may be only a statistical fluctuation.

For both Bennett and Finney models the results according to topological shape are given in Table 5. The trigonal prism with caps is more common than the other 14-faced shape. The Archimedian antiprism with caps is rare; other 16-faced deltahedra are far more common. For most shapes, the counting errors are large because the total number of occurrences is small. The exact numbers of the less common shapes have little significance.

An interesting pattern emerges from these descriptions in terms of deltahedra. For large neighbor distances, the tetrahedra form more than 40% of the volume, and become one multiply-connected region that penetrates the entire volume. A program to find groups at tetrahedra connected face to face, finds one large group which includes most of the tetrahedra present. At the other extreme of small neighbor distance (1.20 or less) it appears that the unenclosed volume forms one multiply-connected interpenetrating region in which the various deltahedra are embedded.

No systematic investigation has been done of the different arrangements of groups of tetrahedra that occur. It is relatively easy to count

TABLE 3

BENNETT MODEL DELTAHEDRA

Faces	Neighbor Distance = 1.30				
	Volume Percent				
	0-200	200-348	348-600	600-1000	1000-1500
4	43.05	37.40	37.42	34.64	34.25
8	12.38	11.65	12.18	10.97	11.49
10	3.47	1.95	1.98	2.18	2.28
12	9.08	10.64	7.92	8.29	5.08
14	3.25	3.41	6.62	3.81	3.97
16	4.07	1.92	4.31	3.64	3.76
18	2.62	2.70	3.68	3.46	2.62
20	1.42	2.09	2.11	2.88	3.13
>20	20.76	28.25	23.79	30.15	33.42

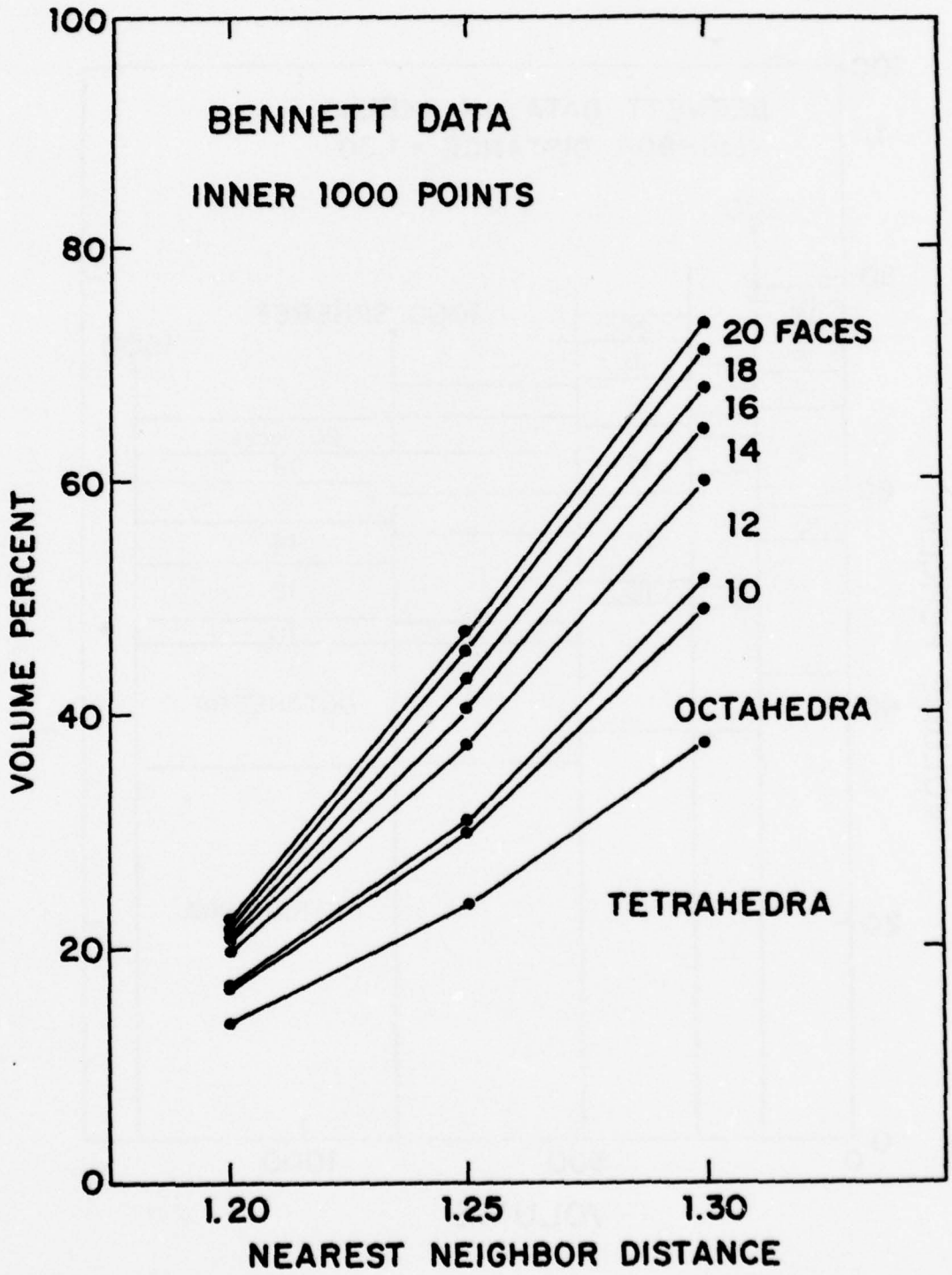

Figure 5b. Volume percentage of various deltahedra in the Bennett model inner 1000 spheres, versus nearest neighbor distance.

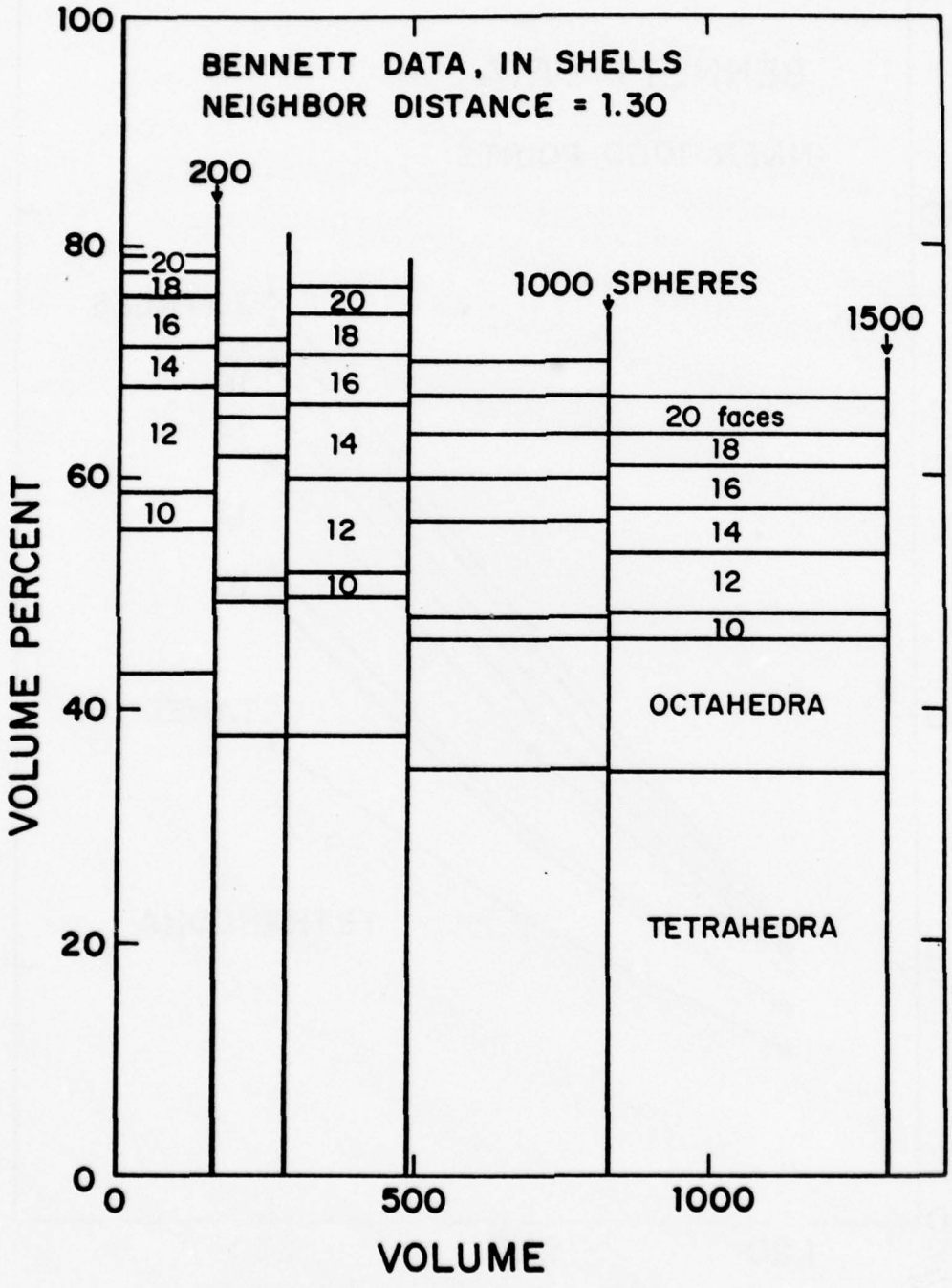

Figure 6. Volume percentage of various deltahedra in the Bennett model, for various shells, with the nearest neighbor distance = 1.30.

TABLE 4

BENNETT MODEL DELTAHEDRA

Faces	INNER 1000 SPHERES					
	Volume Percent			Number per 100 Spheres		
	1.20	1.25	1.30	1.20	1.25	1.30
4	13.71	23.38	37.34	88.2	147.6	231.6
8	2.71	6.17	11.61	4.4	9.8	18.1
10	0.22	1.15	2.34	0.3	1.3	2.6
12	2.83	6.39	8.68	2.5	5.6	7.4
14	0.56	3.09	4.35	0.4	2.1	2.9
16	0.92	2.69	3.64	0.6	1.6	2.1
18	0.77	2.33	3.24	0.4	1.2	1.6
20	0.41	1.49	2.28	0.2	0.7	1.0
>20	77.88	53.32	26.53			

TABLE 5

DELTAHEDRA TOPOLOGICAL TYPES
Number in inner 1000 spheres

Faces	Corner Numbers	N_{6-4}	Finney Model			Bennett Model		
			1.20	1.25	1.30	1.20	1.25	1.30
14	3,6,0		2.2	11.2	17.4	1.0	11.2	15.0
	4,4,1		1.0	3.0	7.9	3.0	9.9	14.3
16	2,8,0			1.1	1.3			
	3,6,1			2.0	1.7		2.2	3.3
	4,4,2	6	1.5	8.0	9.0	3.7	12.0	12.6
	5,2,3		3.0	1.0	1.0	2.0	0.2	4.0
	4,4,2	4	3.0	4.0	1.3		1.5	1.0
18	2,8,1		1.0	1.0	2.0			
	4,4,3	6	0.9	4.1	1.6		2.8	4.9
	4,4,3	7	7.2	11.7	6.2	2.8	7.9	5.8
	4,4,3	9		1.6	0.9	1.0		
	6,0,5			1.0				1.0
	4,5,1,1			2.0	1.0		1.0	4.4
	5,3,2,1							0.05

the rings of five tetrahedra around one edge. With a nearest neighbor distance of 1.20, the Finney model has 61.9 rings (± 8.8 counting error) per 1000 spheres.

4. DESCRIPTION OF STRUCTURAL UNITS: LOCAL ARRANGEMENTS

The previous sections demonstrate that the description in terms of deltahedra does not provide a good description of the local arrangements of spheres; it is not a convenient replacement for Bernal's original description. Too much of the volume is in the large complicated deltahedra. For local arrangement description it is necessary to use shapes with square (four-edged) faces. Three of Bernal's shapes have square faces: square antiprism, trigonal prism and half-octahedron. These can be joined square face to square face to produce large deltahedra. (The square faces need not be capped with half-octahedra). However, most of the deltahedra with 16 or more faces cannot be produced from trigonal prisms, square antiprisms and half-octahedra. Several other distinct local arrangements are required. If we limit the nearest neighbor distance to $\sqrt{12/7}$ or less, we can identify several different local arrangements (in the dense random packing) that have no large interior space and are not topologically equivalent to any of the Bernal holes. Whittaker discovered several of them, but did not propose any exhaustive catalogues of shapes. He reports about 10 miscellaneous unspecified shapes per 100 spheres.

A new catalogue of possible shapes can be prepared allowing faces with three or four edges, but not with five edges. (The "four-edged faces" may be non-planar, in general, and are therefore not called squares

or quadralaterals.) This is similar to Whittaker's approach, but here includes several additional shapes he did not mention. We may first consider only those shapes that cannot be divided into other shapes on the list. All such irreducible shapes with up to eight points are shown in Figure 7. They are:

4 Points: Tetrahedron

5 Points: Half Octahedron
Dihedron (Whittaker's Andalusohedron)
Pentatope (Whittaker's Oblate Trigonal Bipyramid)

6 Points: Trigonal Prism

7 Points: Diploid Heptatope (also called Seven Point Bisymmetric)
Trigonal Heptatope (identified by Whittaker)
(also called Seven Point Trisymmetric)

8 Points: Archimedian Antiprism
Antiprism missing one side edge
Antiprism missing two side edges:
a. with one intervening edge
b. with two intervening edges
c. on opposite sides
Antiprism missing three edges
Cube with one face diagonal
Cube

There are at least 28 topologically distinct arrangements of nine points with 3- and 4-edged faces. Some of them are shown in Figure 9. Many of them may be thought of as being square antiprisms, with one half-octahedral cap, missing one or more edges. There are two sorts of edges on an antiprism: base or top, and side. Removing one side edge creates only a four-edged face, so the shape created remains an eight-point shape.

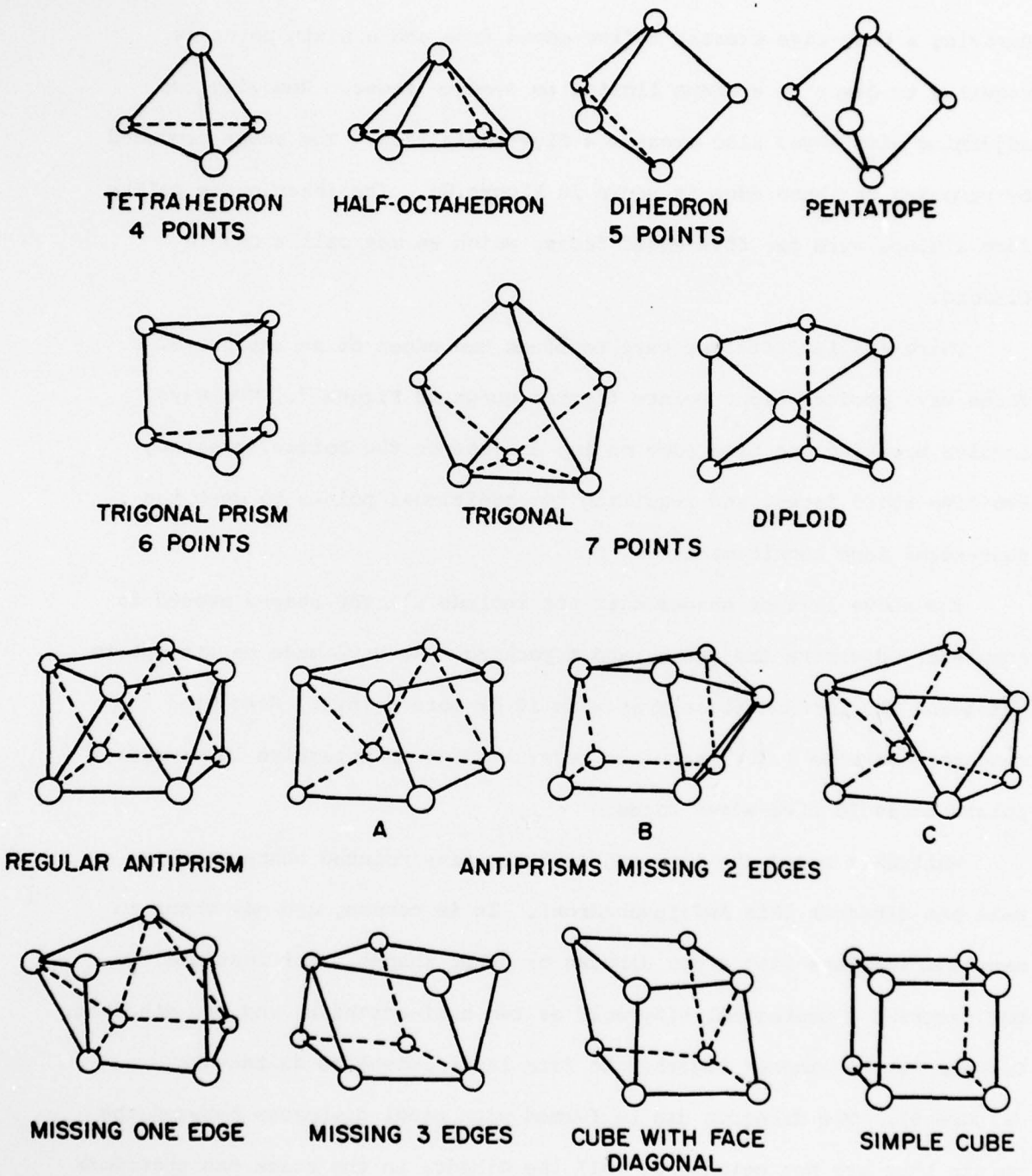

Figure 7. All the irreducible shapes, allowing three- and four-edged faces, with up to eight points.

Removing a base edge creates a five-edged face and a ninth point is required to describe a shape limited to 4-edged faces. Removing two adjoining side edges also creates a five-edged face. The shape produced by removing one base edge is shown in Figure 8a. The inner seven points form a shape with two five-edged faces, which we may call a Double Diamond.

There are 12 different ways to break two edges of an antiprism. Three ways produce eight points figures shown in Figure 7. Two ways involve breaking one base edge on top and one on the bottom, creating two five-edged faces, and requiring two additional points to meet the four-edged face requirement.

The above list of shapes does not include all the shapes needed to completely describe the dense random packing. We have made no attempt to catalogue the irreducible shapes with 10 or more points. Even with the neighbor distance 1.30, there are several sites that require 10 or more points to avoid five-edged faces.

Whittaker noted the importance of the five pointed shape which we call the dihedron (his Andalusohedron). It is common, and may occur in many combinations with other dihedra or other shapes. For instance, we may describe a pentagonal bipyramid as two half-octahedra and one dihedron. Dihedra may be stacked together to form large tube-like deltahedra (Figure 9). The dihedron can be formed with equal distances between the points that are not neighbors. All the dihedra in the stack can therefore be identical. By varying the stacking order, the stack can be either straight or curved. This large deltahedron has no interstitial site larger than that of the single dihedron: center to vertex = 0.69422 (for the equal-diagonal dihedron).

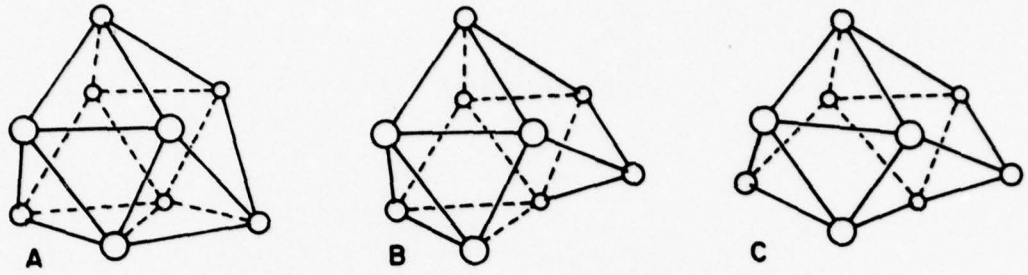

DOUBLE DIAMOND SHAPES

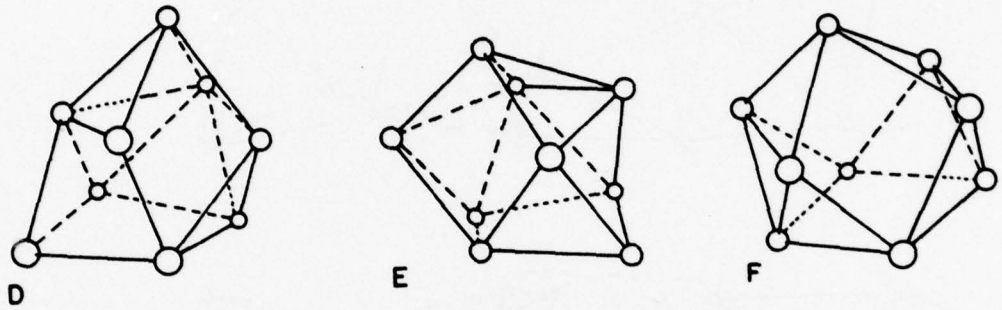

8 TRIANGULAR FACES

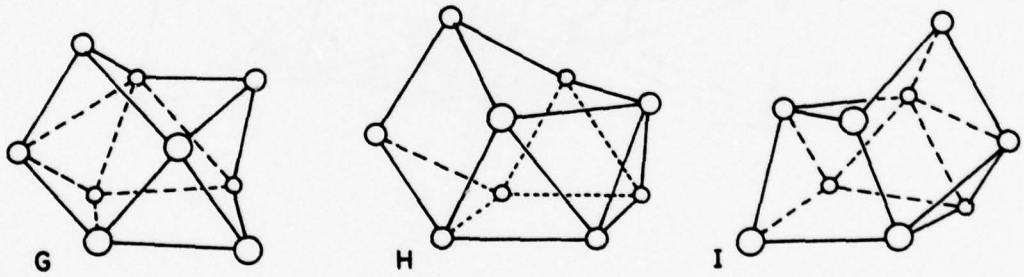

6 TRIANGULAR FACES

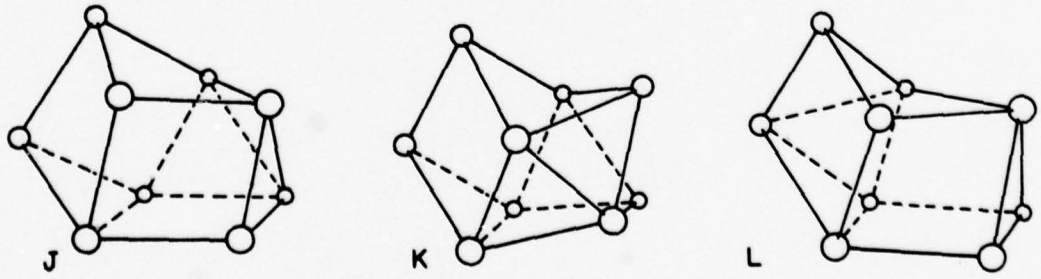

4 TRIANGULAR FACES

NINE POINT SHAPES

Figure 8. Some irreducible shapes with nine points.

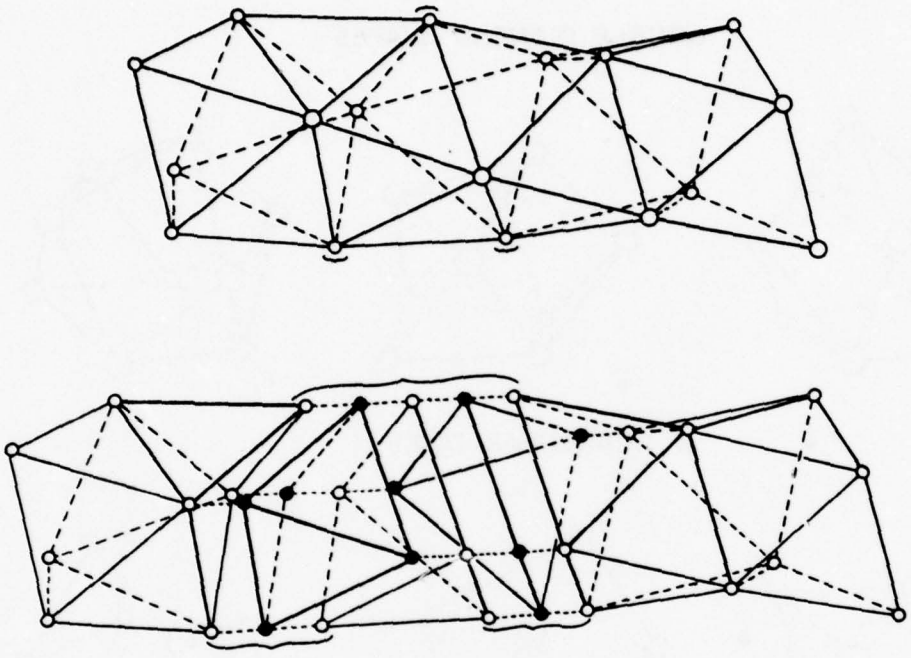

Figure 9. A stack of dihedra, above; and the same stack expanded to show the individual dihedra, below.

All the different shapes may occur with considerable distortion. Figure 10 shows four shapes in extremes that maintain unit edges and symmetry.

In addition to the irreducible shapes, it is interesting to find the statistics for a few other shapes that are reducible but distinct. The list is given in Table 6. All these shapes have intersecting four-edged faces. The octahedron has three. The five other reducible six-point shapes can be thought of as octahedra missing between one and four edges; with two intersecting four-edged faces. This provides a choice of which four-edged face to use to reduce the shape. For all shapes but one the different division choices yield the same types of irreducible shapes. The exception is the Double Dihedron connected, which can be divided into two dihedra, or into a pentatope and a half-octahedron. This difference leads to an ambiguity about the number of pentatopes, dihedra, and half-octahedra present. Fortunately, this shape is rare, so the ambiguity does not seriously affect the statistics observed. Although Whittaker did not discuss this shape, he appears to have found the half-octahedra before searching for dihedra, and would therefore count the shape as a half-octahedron and a pentatope. The four dihedron variations cannot be constructed with all unit length edges and a neighbor distance of $\sqrt{12/7}$ because they would have extra edges and become other shapes.

To correlate local arrangements with deltahedra, Table 7 gives the local shapes that make up various deltahedra with up to 18 faces. Three dihedron variations on which statistics were gathered are shown in Figure 11.

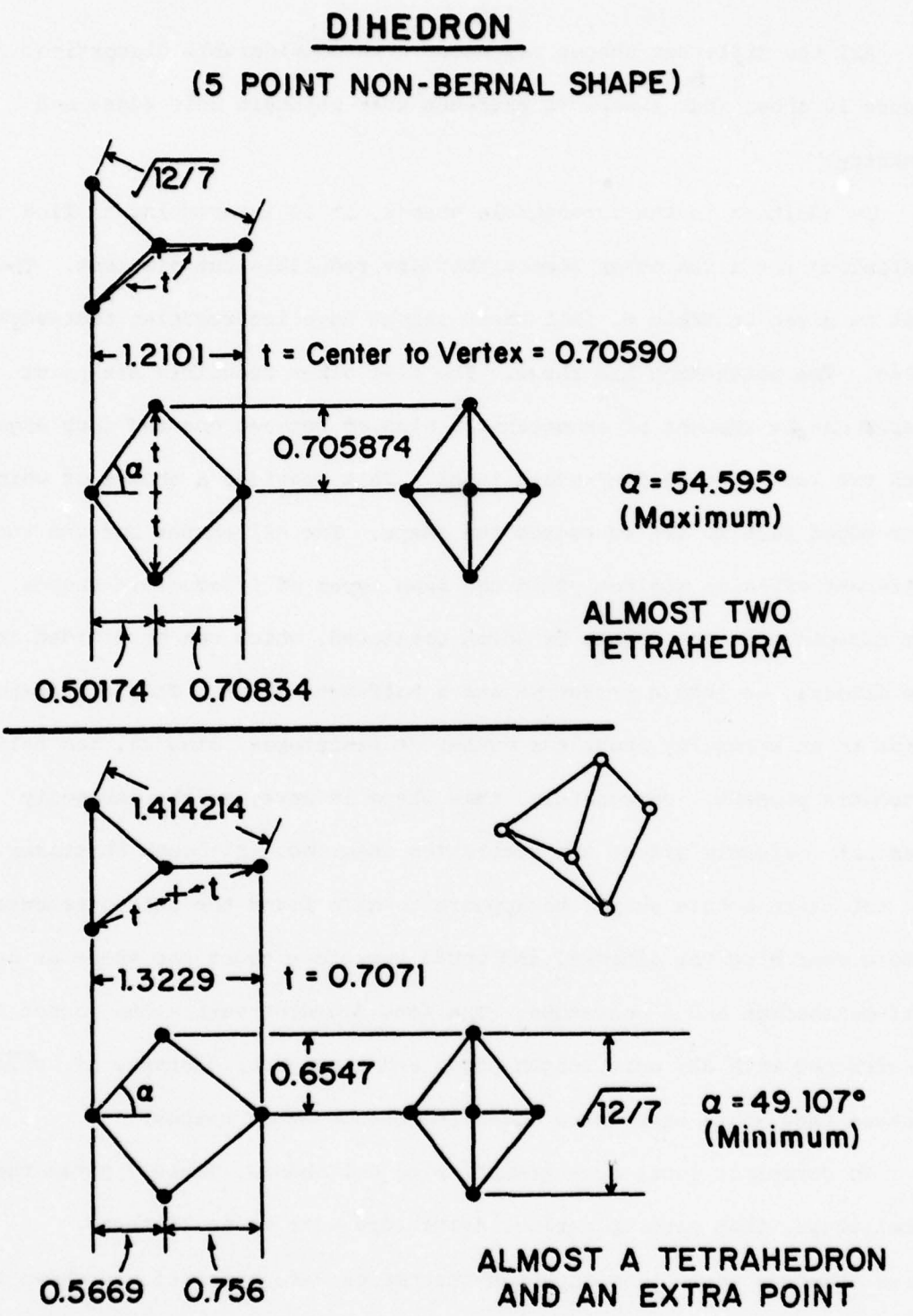

Figure 10a. Simple dihedron, the five-point non-Bernal shape, shown in two extremes that maintain unit edges and symmetry.

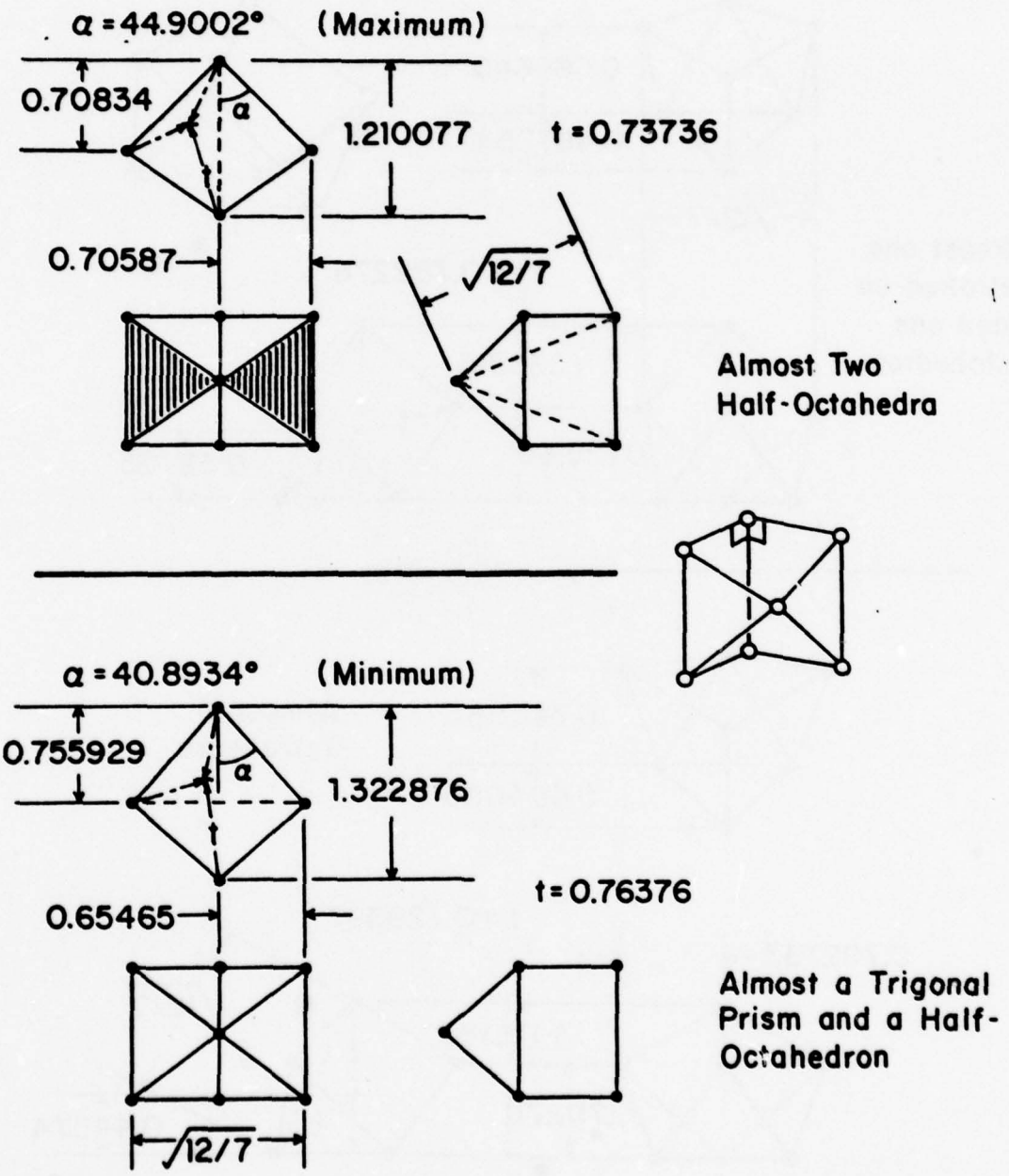

Figure 10b. Bisymmetric Seven-Point shape, shown in two extremes that maintain unit edges and symmetry (called a diploid heptatope in the text).

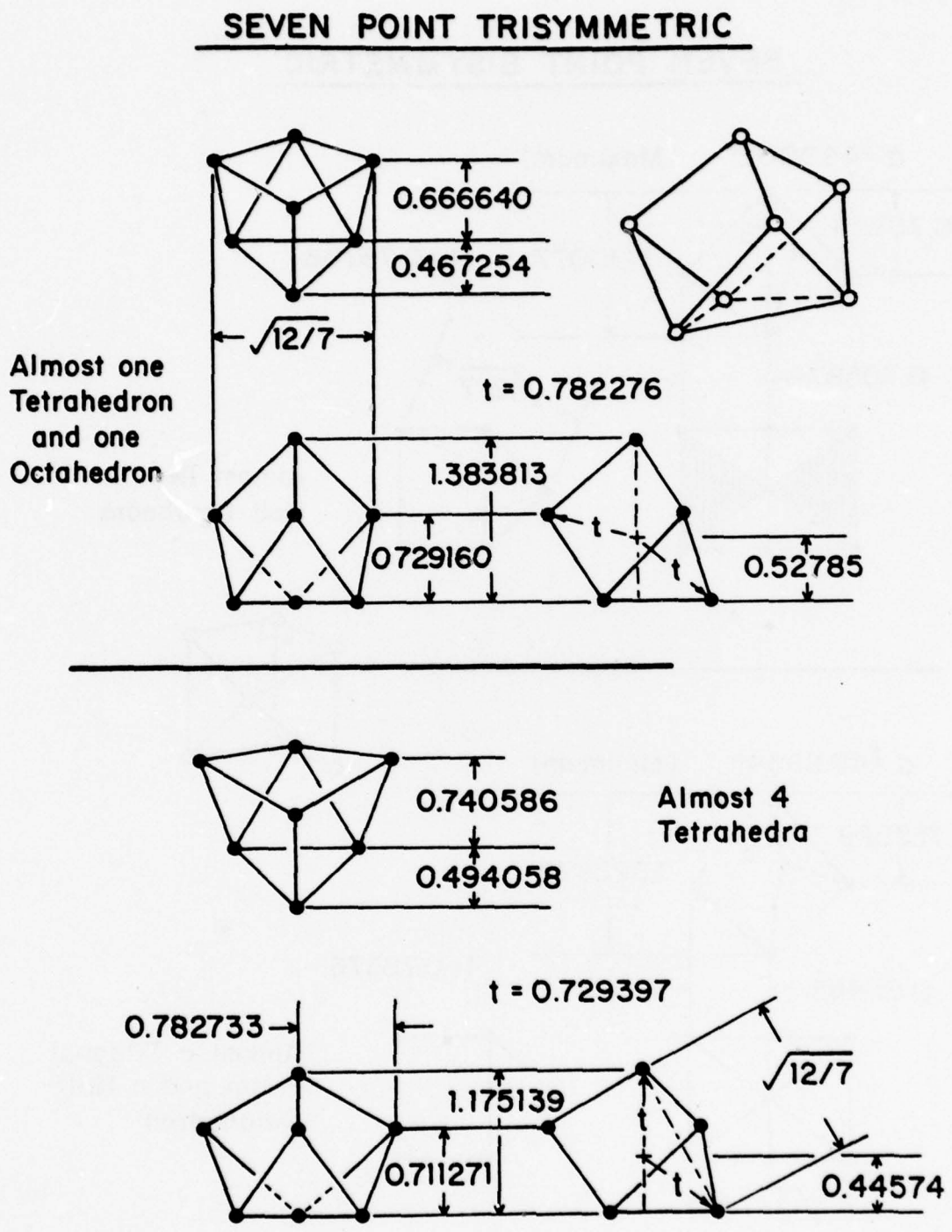

Figure 10c. Trisymmetric Seven-Point shape, shown in two extremes that maintain unit edges and symmetry (called a trigonal heptatope in the text).

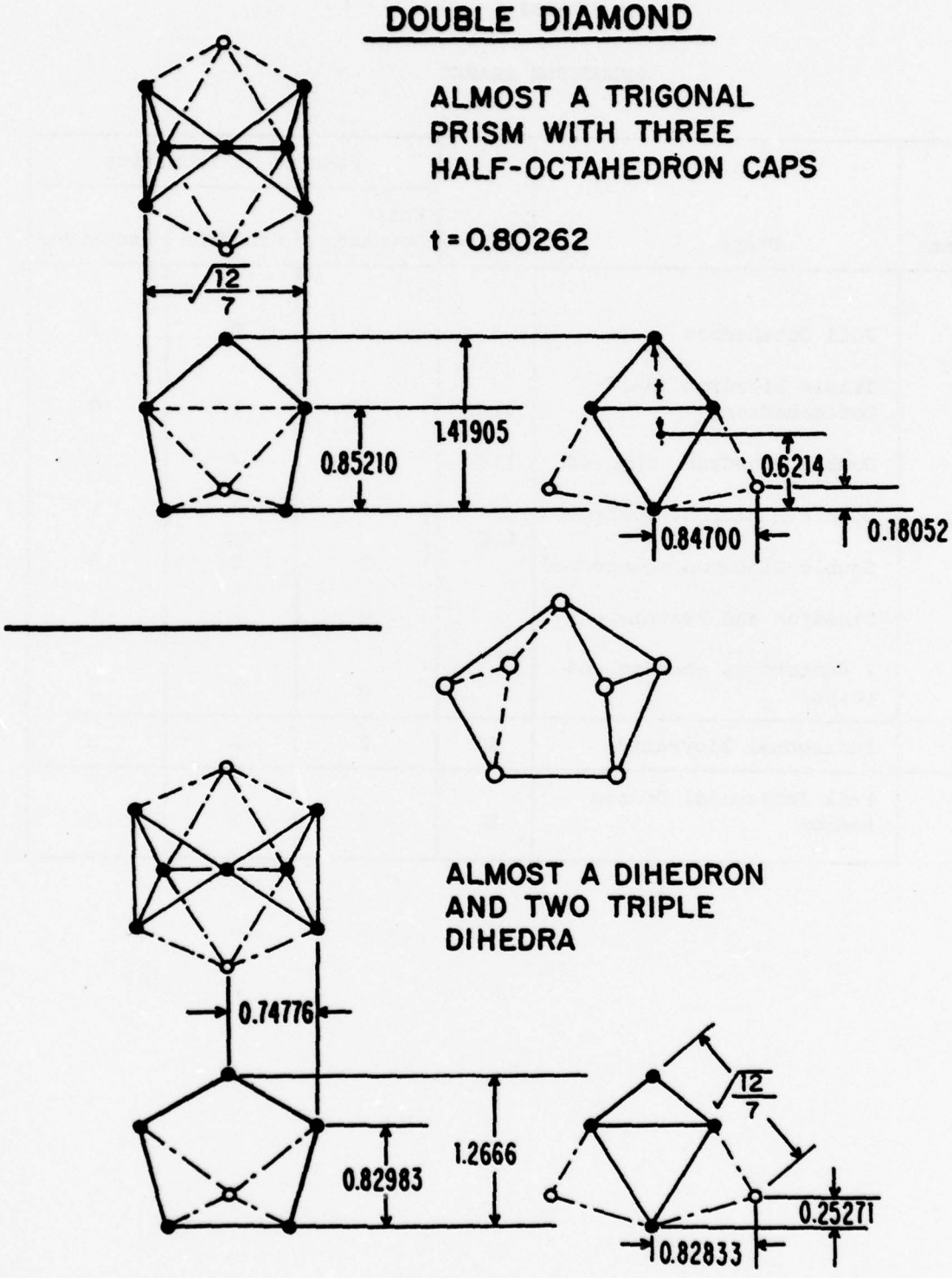

Figure 10d. Double Diamond shape, shown with two auxiliary points, in two extremes that maintain unit edges, symmetry and auxiliary point connections.

TABLE 6

REDUCIBLE SHAPES

Points	Shape	Figure	Results of Reduction		
			Half-Octahedra	Dihedron	Pentatope
6	Full Octahedron	2	2	0	0
	Triple Dihedron (Half-Dodecahedron)	11A	1	1	0
	Double Dihedron, opposed	11B	0	2	0
	Double Dihedron, connected	11C	1	0 or	1
	Double Dihedron, connected		0	2	0
	Dihedron and Pentatope		0	1	1
	2 Pentatopes sharing end points		0	0	2
7	Pentagonal Bipyramid	4A	2	1	0
8	Full Tetragonal Dodecahedron	2	2	2	0

TABLE 7

LOCAL ARRANGEMENTS IN VARIOUS DELTAHEDRA

Deltahedra:	12	14 Faces		16 Faces						18 Faces						
Corners:	4,4,0	3,6,0	4,4,1	2,8,0	3,6,1	4,4,2	4,4,2	4,4,2	5,2,3	2,8,1	4,4,3	4,4,3	4,4,3	4,4,3	6,0,5	4,5,1,1
Local Arrangements / N_{6-4}						4	6*	6			6	7	8*	9		
Half Octahedron		3		2	3			2		2		2	4	2		
Trigonal Prism		1						1				1				
Archimedian Antiprism				1												
Single Dihedra			1				2				3	1				3
Pentatope															1	
Triple Dihedra	2		2			2	2	1	2		2	1		1	3	2
Double Dihedra (connected)									1							
Double Dihedra (opposed)						1										
Seven-Point Bisymmetric													1			
Seven-Point Trisymmetric					1									1		
Double Diamond										1						

*Not found, nor shown in Figure

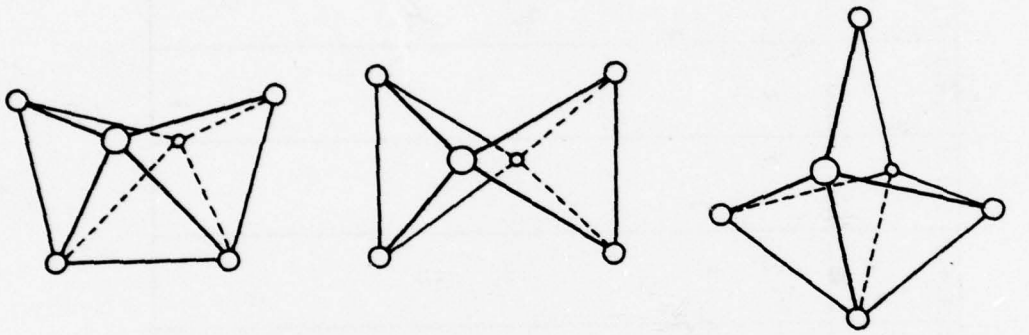

Figure 11. Variants of the dihedron.

a. Triple Dihedron
b. Double Dihedron (opposed)
c. Double Dihedron (connected)

5. LOCAL ARRANGEMENT STATISTICS

The numbers of each local arrangement were found for the Finney model and the Bennett model for neighbor distances of 1.20 and 1.30. Examples of all possible irreducible shapes with eight or fewer points were discovered. For the irreducible shape statistics, a double dihedron connected is counted as a half-octahedron and a pentatope. The results are reported in Table 8 as the number of shapes per 100 spheres. Volume statistics were not calculated because of the ambiguity of volume for shapes with non-planar four-edged faces. Instead of fractional volume, therefore, the fractional number of points inside the given cluster boundary was used as the fractional contribution to the total statistics reported. For the various nine point figures, the total number of each type discovered is given in Table 9.

The first 12 shapes in Table 8 were found by various programs that found all occurrences of that shape. To find shapes with nine or more points, we resorted to investigating the largest interstitial sites within 8.0 sphere diameters of the center: the largest 400 sites for the Finney model, the largest 200 for the Bennett model. This procedure might miss some occurrences of the shapes. The statistics for large shapes at 1.20 neighbor distance are only approximate. We believe that we have found all or nearly all the shapes at neighbor distance 1.30. We have probably missed a few shapes at 1.20. The statistics in Table 8 for the Bennett model are for the inner 1000 spheres. With minor exceptions, no other sample size is reported. The statistics should vary with cluster radius, as the deltahedra statistics do, because the density varies with radius. For the Finney model, various sample sizes were used, because presumably the structure does not depend on radius.

TABLE 8

LOCAL ARRANGEMENT STATISTICS
(shapes per 100 spheres)

Irreducible Shapes:	Bernal (Whittaker) 1.20	Finney 1.20	Bennett (Inner 1000) 1.20	Finney 1.30	Bennett (Inner 1000) 1.30
Tetrahedra	116 ± 4	121.4 ±3.5*	88.2 ±3.0**	249.6 ±5.0*	231.6 ± 4.8**
Half-Octahedra (All)	61	85.6	70.9	100.6	97.9
Dihedra (All) (Andalusohedra)	110	98.0	115.6	57.1	72.2
Pentatopes (All) (Oblate Trigonal Bipyramids	5 ± 1	9.7 ±0.98	14.3 ±1.2	0.4 ±0.3	2.34 ± 0.48
Trigonal Prisms	12 ± 2	12.7 ±1.1	18.7 ±1.4	5.3 ±1+	9.8 ± 1.0
Trigonal Heptatopes	4 ± 1	3.24±0.57	4.37±0.66	1.57±0.56	2.6 ± 0.6
Diploid Heptatopes	Not reported	1.30±0.36	5.3 ±0.73	0.38±0.12++	0.8 ± 0.3
Archimedian (square) Antiprisms	~0	0.2 ±0.1	0.55±0.23	0.35±0.12	0.5 ± 0.2
Antiprisms missing one edge	~10	1.62±0.4	1.46±0.38	0.3 ±0.2	0.4 ± 0.2
Antiprisms missing two edges: a		0.78±0.28	1.89±0.43	0.08±0.05++	0.12 ± 0.07++
b		0.2 ±0.1	0.3 ±0.2	0.04±0.04++	0
c		0.1 ±0.1	0.1 ±0.1	0	0.12 ± 0.07++
Antiprisms missing three edges		0.04±0.04++	~0	0.04±0.04++	~0
Cube with Face Diagonal		0.08±0.08++	0.2 ±0.1	0.04±0.04++	~0
Simple Cube		0	0.1 ±0.1	0	0
Nine-Point Shapes		1.54±0.24++	0.3 ±0.2	0.92±0.19++	0.3
More than Nine Point Shapes		4.54±0.42++	2.1 ±0.5	1.04±0.20++	0.2

TABLE 8 continued

Other Shapes:	Bernal (Whittaker) 1.20	Finney 1.20	Bennet (Inner 1000) 1.20	Finney 1.30	Bennett (Inner 1000) 1.30
Full Octahedra	7 ± 1	10.7 ±1.03*	4.39±0.66**	24.7 ±1.6*	18.1 ±1.35**
Isolated Half Octahedra	27 ± 2	27.3 ±1.65	28.6 ±1.69	18.4 ±1.9	20.1 ±1.4
Full Dodecahedra	3 ± 0.4	4.53±0.67*	2.50±0.5**	7.9 ±0.9*	7.4 ±0.9**
Isolated Triple Dihedra (Half-Docahedra)	24 ± 2	23.6†	22.2†	14.2†	21.0†
All Triple Dihedra	30‡	32.7 ±1.8	27.2 ±1.65	30.0 ±2.4+	35.8 ±1.9
Isolated Dihedra	Not reported	58.9 ±2.4	83.4 ±2.89	25.0 ±2.2	36.3 ±1.9
Dihedra except those in Triple Dihedra	80 ± 3	65.3	88.4	27.1	39.5
Double Dihedra Connected	Not reported	3.55±0.6	5.68±0.75	0.17±0.1+	1.25±0.35
Double Dihedra Opposed	Not reported	3.02±0.55	2.35±0.48	0.43±0.3+	0.63±0.25
Pentagonal Bipyramids	Not reported	0.4 ±0.2	0.29±0.17	1.29±0.5+	2.44±0.49
Double Diamonds	Not reported	2.39±0.49	1.86±0.43	1.77±0.6	0.5 ±0.2

NOTES:

*Deltahedra numbers, Table 2

**Deltahedra, inner 1000 spheres, Table 4

+Inner 500 spheres

++Inner 2600 spheres

†Calculated from: All Triple Dihedra - 2 × Full Dodecahedra

‡Calculated from: Isolated Half-Dodecahedra + 2 × Full Dodecahedra

TABLE 9

NINE-POINT SHAPES
Total Number Discovered
(Inner 2600 Spheres)

Shape (Figure 8)	Finney 1.20	Bennett 1.20	Finney 1.30	Bennett 1.30
A	6	0	9	4
B	4	2	7	5
C	5	4	0	1
D	3	0	1	0
E	5	4	1	3
F	2	0	2	0
G	2	1	1	0
H	4	2	1	1
I	2	0	1	0
J	4	4	1	1
K	1	3	0	0
L	0	1	0	0
Others not in Figure 8	2	0	0	0

There are some unexpected differences between our results on the Finney model and Whittaker's results on the Bernal model. We originally expected these two models to be almost identical because they appear to be similarly constructed. The statistically significant differences are in pentatopes, (Bernal 5 ± 1, Finney 9.7 ± 1.0) and full octahedra (Bernal 7 ± 1, Finney 10.66 ± 1.03). The two models differ in other statistics but not by much more than the expected counting errors. These differences introduce the intriguing possibility that not all mechanical hard-sphere dense random packings are identical. This study sheds little light on how the two models might be different. Perhaps the surface effects penetrate a significant distance into the cluster, which affected the Bernal core more than the Finney core. Perhaps a mechanical model changes its statistics when deformed or thoroughly shaken. We did expect differences between the Finney and Bennett models because they were differently constructed. The significant differences are that the Bennett model has fewer tetrahedra and complete octahedra, and more dihedra, pentatopes, and trigonal prisms. At a neighbor distance of 1.20, the Bennett model has more diploid heptatopes.

6. INTERSTITIAL SPHERE SIZES

Another approach to the describing the holes between spheres of a dense random packing is to enumerate how many interstitial spheres of what size could be placed in the holes between the unit spheres. Polk[7] speculated that the structure of metal-metalloid glasses may have the metal atoms in a dense random packing, with the metalloid atoms at the interstitial sites of the larger Bernal holes (trigonal prisms and

Archimedian antiprisms). Polk and Cargill point out that the regular Bernal shapes are not large enough for the metalloids, but the Bernal shapes are distorted in the actual dense random packing, and other shapes also occur. We shall find that the distortions do not increase the size of the larger interstitial sites.

We must be careful in defining our interstitial site statistics. Any four non-coplanar points (unit sphere centers) define a sphere. If no other point is inside that sphere, then that sphere represents an interstitial site. A small sphere could be placed there that would touch each of the four unit spheres and none others. It is possible, however, to arrange the unit spheres in such a way that one small interstitial sphere would overlap with a neighboring small interstitial sphere. It is unreasonable to count both such interstitial sites in the statistics. If only two overlap, then we should take the larger and neglect the smaller. It would be possible, though more difficult, to redefine the smaller site, as a still smaller site for a sphere that just touches three unit spheres and the larger interstitial sphere. This has not been attempted. If three sites overlap, with the center the largest, but the other two not overlapping each other, then we must choose between the maximum number of sites (using the two smaller) and the maximum size of sites (the one largest). We have chosen the latter.

The approach used was to find all interstitial sites, sort them by size, and then eliminate overlap from the largest down. That is, choose the largest unchosen site and eliminate from the remaining (unchosen) list any site that it overlapped.

The results of this analysis for the inner core of the Finney Model are shown in Figure 12. There are very few sites larger than the one in a regular Archimedian antiprism, 0.8227. None is larger than 0.85, which is smaller than the site in a simple cube (0.8660).

The same results are replotted in Figure 13, showing the total integrated number of sites that are equal or larger than a given center to vertex distance. Also shown are the results obtained from Bernal's numbers, using the numbers of shapes derived by Cargill, and assuming undeformed shapes. The actual array has more larger sites than the simple model, but not significantly more. If we were to adequately describe a metal-metalloid glass as a dense random packing of single-sized spheres for the metal atoms, with the metalloid atoms occupying interstitial sites, then the metalloid must be small enough, or scarce enough to fit into the available sites. For a typical 80 metal - 20 metalloid glass, we would need 25 sites per 100 metal spheres. Figure 13 indicates that to have that many sites, we would need sites as small as 0.74 (center to vertex distance). The sphere in such a site has a diameter 0.48 that of the unit sphere. Even with 91 metal - 9 metalloid, the interstitial sphere diameter would have to be as small as 0.54. This is substantially smaller than the metalloid sizes derived from X-ray studies. Unfortunately, this study does not provide information of what the correct metal atom packing is.

The same analysis of interstitial sites was done on the Bennett Model. Since the density varies with distance from the cluster center, the interstitial site statistics also vary. As expected, at lower densities there are more large sites and fewer small sites. Figure 14

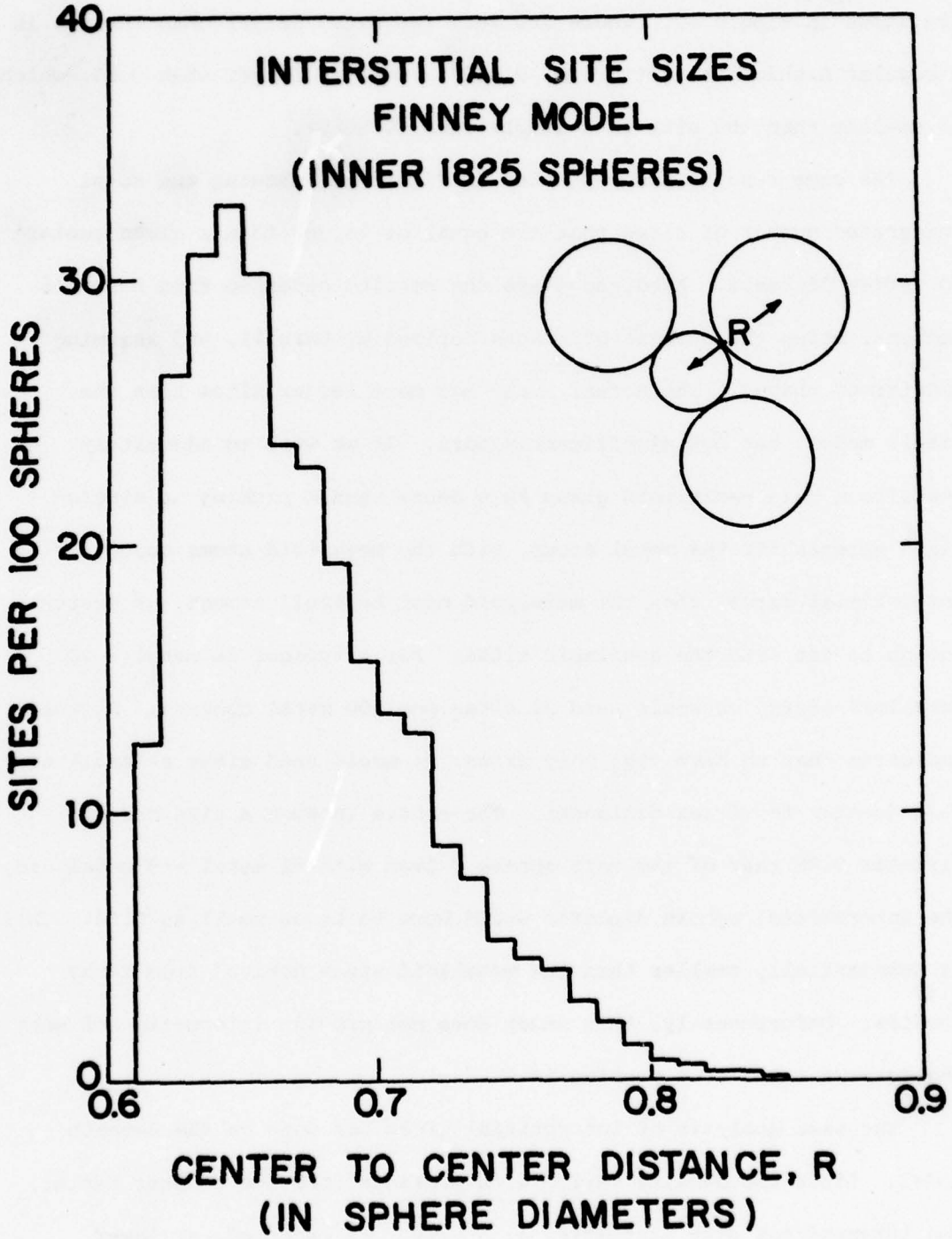

Figure 12. Interstitial sphere sizes in the Finney Model.

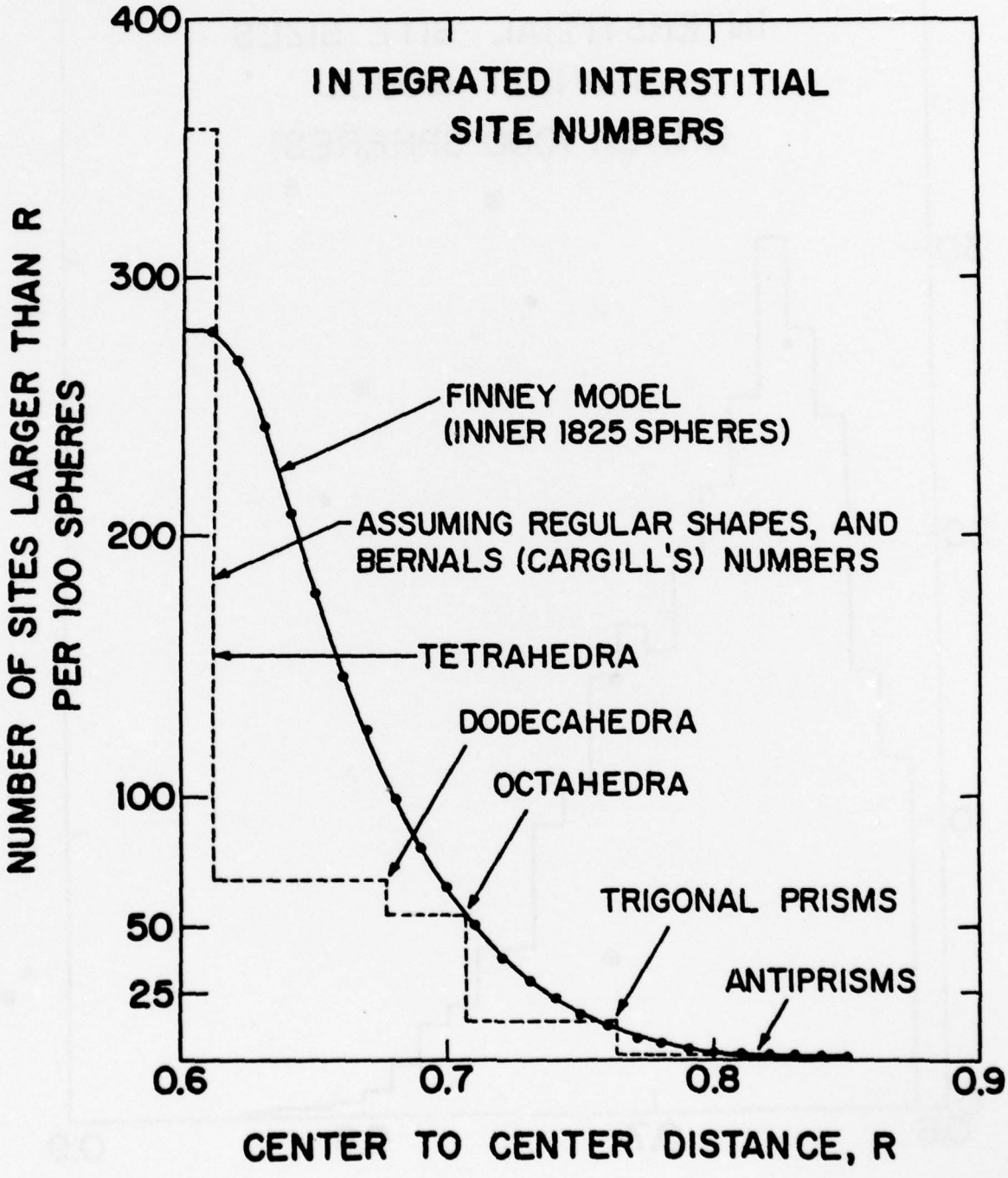

Figure 13. Integrated number of interstitial spheres greater than or equal to various sizes, Finney Model.

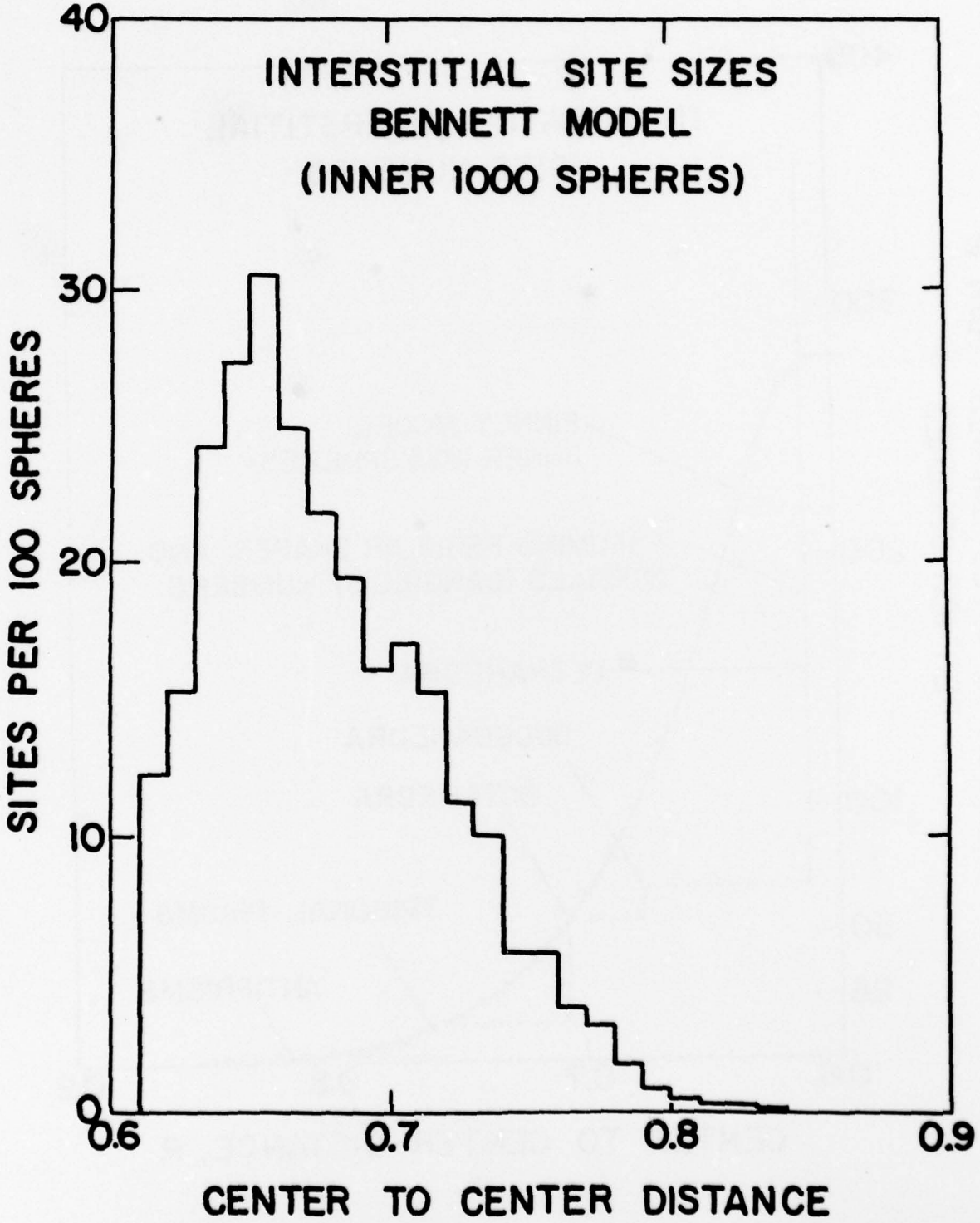

Figure 14. Interstitial sphere sizes in the inner 1000 spheres of the Bennett Model.

gives the results for the inner 1000 spheres. The average density of this cluster is about the same as the Finney Model, and the site statistics are about the same also.

7. CONCLUSIONS

Two different models of a dense random packing of the hard spheres have been analyzed in terms of the polyhedral holes between spheres: The Finney mechanical model and the Bennett computer generated model. An accurate and unambiguous description of the structure requires more different structural units than Bernal[1] originally proposed. A description in terms of deltahedra (triangular-faced polyhedra) yields a significant volume fraction of large and complicated shapes.

The packings were also described in terms of local arrangements allowing three and four-edged faces. All such shapes with up to nine points were considered, including those used by Whittaker[6] to describe Bernals model, plus several others. Although there are occasional sites that must be described with shapes of 10 or more points, the local arrangement list provides a manageable way to describe most of the volume.

Both models were also analyzed to find the number and size of the small spheres that could be placed at the interstitial sites. The results confirm that there are not enough large sites in the packing to allow a model of a metal-metalloid glass to be constructed simply by inserting small spheres into the interstices.

ACKNOWLEDGEMENTS

The author thanks C.H. Bennett and J.L. Finney for permission to use the coordinates of their respective dense random packing models. He also thanks G.S. Cargill for supplying the coordinates of the Finney model. Special thanks are due to Professor F. Spaepen and Professor David Turnbull for frequent help. This work has been supported by the Office of Naval Research under Contract No. N00014-77-C-0002, and by the National Science Foundation under Contract No. NSF-DMR77-10151.

REFERENCES

1. J.D. Bernal, Proc. Roy. Soc. 280A, 299, (1964).

2. J.L. Finney, Proc. Roy. Soc. 319A, 479, (1970).

3. G.D. Scott, Nature 188, 910, (1960); 194, 956, (1962).
   G.D. Scott and D.L. Mader, Nature 201, 382, (1964).

4. Charles H. Bennett, J. Appl. Phys. 43, 2727, (1972).

5. G.S. Cargill III, Solid State Physics 30, 227, (1975).

6. E.J.W. Whittaker, J. Non-Crystalline Solids 28, 293, (1978).

7. D.E. Polk, Acta Met. 20, 485, (1972).

APPENDIX: COMPUTING PROCEDURES

A. Deltahedra

The computer program used to determine the deltahedra is straightforward, but not trivial. First, all nearest neighbor pairs were found, each pair becoming a numbered edge. Then all edges were searched to find all groups of three in a triangle, which become numbered faces. It is necessary to cross-reference which edges border each face, and which points and which faces border a given edge. All faces are then searched to identify all groups of four forming a tetrahedron. A more sophisticated search then identifies all the larger holes. It requires keeping track of which side of each face is being searched, using the numbers of the three points of the face to define a right-handed and a left-handed side. The search proceeds from face to face, choosing the next face as that which forms the smallest interior angle about the joining edge. This search continues for a given hole until there remain no edges of the faces in the hole that are not connections to other faces in the hole. Special provision must be made to identify interior faces that have free edges.

The exterior of the cluster is treated by this program as one very large hole, which is excluded from the statistics.

To get good statistics on the volume fractions of the various types of holes one must avoid surface effects and consider only the holes and volume within an inner core (usually 1000 spheres). The volume of each hole that was within this inner cluster boundary sphere was used for the volume fraction calculation. For the holes that crossed the boundary

sphere, an approximate calculation of the fraction of volume within the boundary sphere was done.

The volume of each hole was calculated as a group of tetrahedra with the common vertex being the vertex closest to the origin. Each tetrahedra was truncated by its intersection with the boundary sphere. The truncated faces were considered to be flat, not rounded like the boundary sphere. There are four possible cases here: One, two, three or none of the three points of the face outside the boundary sphere. With none outside the whole tetrahedron is used. When all three are outside the truncated face is a triangle and used directly. If one or two points are outside the truncation forms two faces: a triangle and a quadrilateral as shown in Figure A-1.

This approximate volume calculation at the cluster boundary introduces a small systematic error. If all the volume of the cluster were assigned to different deltahedra, the total volume recorded would not be that of the sphere, but of a many-faced polyhedron inscribed inside that sphere. The volume percentages were calculated using the volume of the cluster sphere, not the inscribed polyhedron, and are therefore slightly lower than an exact calculation. The volume of the inscribed polyhedron is usually not known, because not all volume within the cluster boundary is assigned to deltahedra, even when all spheres are considered out to 2.5 sphere diameters beyond the cluster boundary. These errors are small compared to the statistical counting errors involved, which are shown for 2000 points.

For all deltahedra with eleven or fewer corners, a subroutine was used to find the particular topological type. The number of faces

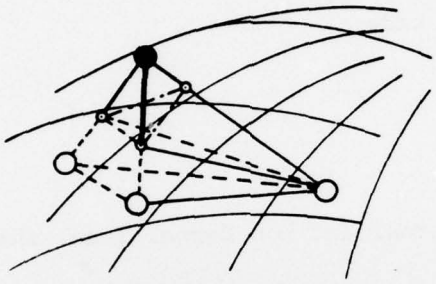

ONE POINT OUTSIDE

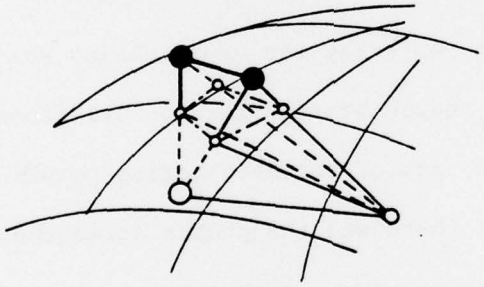

TWO POINTS OUTSIDE

Figure A-1.

touching a particular corner was found by searching through all the faces on the hole. This was done for each corner.

Groups of tetrahedra were found in a straightforward manner, searching each face on a tetrahedron to see if another tetrahedron was on the other side. This search was continued for a particular group until there remained no faces in the group that had an unidentified tetrahedron on the other side.

B. Local Arrangements

To search for the Bernal and non-Bernal local shapes various different programs were used. All were based on finding edges and faces in the manner described above.

To find trigonal prisms, an array was used telling which faces touched a given point. The search started through all faces. For each face, all faces that touched each of the neighboring points of the first point were checked to see if there was the proper arrangement of neighbors between the two faces: i.e., each point on each face neighbors one and only one point on the other face.

The program to find Archimedian antiprisms searched from face to face until the proper circuit had been discovered. The procedure is slow because of the great number of possibilities.

The program to find dihedra is rather simple. The program first looped over all edges. Up to six faces may meet at an edge. For each edge, the program checked each different pair of faces that meet at that edge. The two points on those faces that don't touch the edge are picked out as extremal points. (If the extremal points are neighbors, the shape

is a tetrahedron, and that pair of faces can be neglected.) All points that neighbor both extremal points are then found. (Two of these are the ends of the base edge.) If no such mutual neighbors (other than the base edge points) are found, the pair of faces is neglected. The actual shape represented by the pair of faces is determined by the number of mutual neighbors and whether they neighbor each other and the base edge points. The various possibilities are easy to identify, but care must be used to correct for multiple counting. A pentagonal bipyramid will be discovered five different times by this program. A double dihedron, either connected or opposed, will be discovered twice. A triple dihedron could be discovered either from a central base edge, or from the two side edges. The second type of discovery is neglected. A complete octahedron will be discovered by this program twelve different times. To find half octahedra is more difficult, because we must distinguish between individual isolated half-octahedra, and the half-octahedral parts of triple dihedra, double dihedra connected, and pentagonal bipyramids. To do this, we first identify the two points of the half-octahedron that would form the diagonal perpendicular to the diagonal formed by the two extremal points. One of these points is the mutual neighbor discovered, and the other is the base edge point that doesn't neighbor the mutual neighbor. We then search for mutual neighbors of these two diagonal points. If there are only three such mutual neighbors, the shape is indeed an isolated half-octahedron. If there are four it is a double or triple dihedron; if five, it is a pentagonal bipyramid. Each half-octahedron will be discovered four different times.

To find the trisymmetric seven point figures, the program considered, for each face, all the various combinations of three neighboring faces,

one on each edge. The three outside points were identified (those not on the central face). If any two (or three) outside points were identical, the shape was rejected as a tetrahedron. If any two (or three) were neighbors, the shape was rejected as a half-octahedron or something related. If no outside points were identical or neighbors, the program searched for points that neighbored all three. If none or two or more were found the shape was rejected. If only one point was found (the seventh point of the shape), it was checked to see whether it neighbored any of the three points of the base triangle. If it did, the shape was rejected. If it didn't, the shape was a seven-point tri-symmetric shape (trigonal heptatope).

A program was written to identify the seven-point bisymmetric shapes (dipbid heptatopes), which searched through all pairs of faces meeting at a point to find the correct arrangement of points.

A program to find the various larger local arrangements was attached to the program for dihedra. If no mutual neighbors were discovered for the extremal points of a pair of faces, then a search was made for a pair of points (e.g., I5 and I6 in Figure A-2a) that neighbored each other, one neighbored each extremal point (I3 and I4), and neither neighbored either base edge point. There can be more than one I5 or I6 to satisfy these conditions, so we may find double diamond shapes directly (e.g., Fig. A-2b). Each double diamond shape will be found twice.

If we find only one I5 and one I6, we may proceed to find other shapes by looking for I7 and I8 (Figure A-2c): points which neighbor

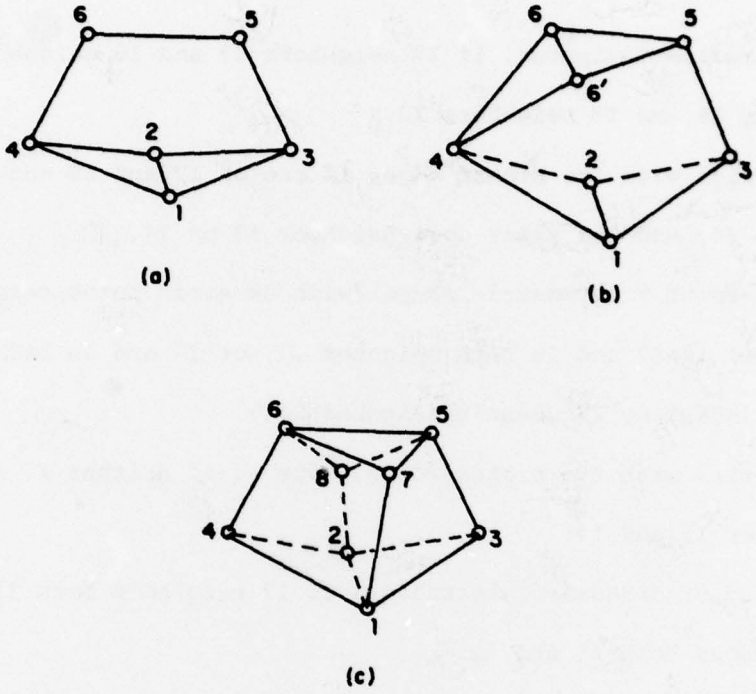

Figure A-2

both I5 and I6 and also neighbor I1 and I2, respectively. If we find both I7 and I8, we have found one of the five following local arrangements.

1. Archimedian Antiprism, if I7 neighbors I3 and I8 neighbors I4, or I7 neighbors I4 and I8 neighbors I3.

2. Antiprism with one broken edge, if one of I7 and I8 neighbors neither I3 nor I4, and the other does neighbor I3 or I4.

3. Seven-Point Trisymmetric shape (with an extra point capping a foud-edged face) if I7 and I8 both neighbor I3, or I7 and I8 both neighbor I4. (Assuming I7 doesn't neighbor I8.)

4. Antiprism with two broken edges, Type C, if neither I7 nor I8 neighbors either I3 and I4.

5. A group of dihedra or tetrahedra if I7 neighbors both I1 and I2 or I8 neighbors both I1 and I2.

If we fail to find either I7 or I8, we may be looking at one of the shapes mentioned above from a different base edge. This may be checked using the numbers of the points involved. If the same points form a standard figure elsewhere, we use that standard identification.

Occasionally, the failure to find I7 or I8 represents an antiprism with two missing edges. To help sort out which type it might be, the program will find all points that neighbor both I5 and I1, I5 and I2, I6 and I1, and I6 and I2. The exact shape must often be reconstructed by inspection, using a short program which will report all the neighbors of any particular point.

Some of the more complex shapes reported will not be found by any of the special programs just described. These were identified by plotting a projection of the points within 1.5 of each of 400 largest interstitial sites within 8.0 sphere diameters of the center of the Finney model (center to vertex distance greater than 0.752(and identifying by inspection the shape that surrounded the interstitial site. This was also done for the largest 200 sites of the Bennett model (center to vertex 0.774).

C. Interstitial Sites

A potential interstitial site is equidistant from four sphere centers, with no other sphere closer. To find all such sites, we must consider all combinations of four spheres, and check that no fifth sphere overlaps. This leads to calculation times proportional to the fourth (or fifth) power of number of spheres, unless some restrictions on combinations are used. Preliminary calculations found no sites with center to vertex distance greater than 0.85. The main program, therefore, neglected most combinations of four spheres with any two more distant than 1.8. With this restriction, sites larger than 0.90 might be neglected.

For computing convenience, the array was first distributed to unit cells, and the spheres in each cell were recorded in an array. The interstitial sites in each unit cell were found using the points in that cell and the 26 neighboring cells. Each combination of four points (not more than 1.8 distant) was used to calculate a sphere center and radius. If the center was outside the unit cell or the radius was larger than

0.90, that combination was neglected. Otherwise the site was checked for overlap with all other spheres in the 27 cells.

The calculation was done for all cells not totally outside a radius of 8.0 from the center of the array. The array used was the central 4000 points (or 3999 for the Bennett model), which includes all points within 9.2301 of the center (9.2799 for Bennett). After finding all the sites, those at radii greater than 8.0 were excluded to avoid false sites at the edge of the array. Using these sites, the elimination of overlaps was done, leaving an array of far fewer interstitial sites.

Of these sites, those within a radius of 7.1 were used for statistics, to avoid counting sites that avoided being eliminated by overlap because they were near the cluster surface. In the Finney model there are 1825 points inside that radius. The results for the Bennett model depend on radius and are reported for the inner 1000 points, or inside a radius of 5.82625.

Defense Documentation Center
Cameron Station
Alexandria, Virginia 22314 (12)

Office of Naval Research
Department of the Navy
Attn: Code 471 (3)
Code 105 (6)
Code 470

Director
Office of Naval Research
Branch Office
495 Summer Street
Boston, Massachusetts 02210

Director
Office of Naval Research
Branch Office
536 South Clark Street
Chicago, Illinois 60605

Office of Naval Research
San Francisco Area Office
760 Market Street, Room 447
San Francisco, California 94102

Naval Research Laboratory
Washington, D.C. 20390
Attn: Code 6000
Code 6100
Code 6300
Code 6400
Code 2627 (6)

Attn: Mr. F.S. Williams
Naval Air Development Center
Code 302
Warminster, Pennsylvania 18974

Naval Air Propulsion Test Center
Trenton, New Jersey 08628
Attn: Library

Naval Weapons Laboratory
Dahlgren, Virginia 22448
Attn: Research Division

Naval Construction Battalion
Civil Engineering Laboratory
Port Hueneme, California 93043
Attn: Materials Division

Naval Electronics Laboratory Center
San Diego, California 92152
Attn: Electronic Materials Sciences Div.

Naval Missile Center
Materials Consultant
Code 3312-1
Point Mugu, California 93041

Commanding Officer
Naval Ordnance Laboratory
White Oak
Silver Spring, Maryland 20910
Attn: Library

Naval Ship R. and D. Center
Materials Department
Annapolis, Maryland 21402

Naval Undersea Center
San Diego, California 92132
Attn: Library

Naval Underwater System Center
Newport, Rhode Island 02840
Attn: Library

Naval Weapons Center
China Lake, California 93555
Attn: Library

Naval Postgraduate School
Monterey, California 93940
Attn: Materials Sciences Dept.

Naval Air Systems Command
Washington, D.C. 20360
Attn: Code 52031
Code 52032
Code 320

Naval Sea System Command
Washington, D.C. 20362
Attn: Code 035

Naval Facilities
Engineering Command
Alexandria, Virginia 22331
Attn: Code 03

Scientific Advisor
Commandant of the Marine Corps
Washington, D.C. 20380
Attn: Code AX

Naval Ship Engineering Center
Department of the Navy
Washington, D.C. 20360
Attn: Director, Materials Sciences

Army Research Office
Box CM, Duke Station
Durham, North Carolina 27706
Attn: Metallurgy and Ceramics Div.

Army Materials and Mechanics
Research Center
Watertown, Massachusetts 02172
Attn: Res. Programs Office (AMXMR-P)

Commanding General
Department of the Army
Frankford Arsenal
Philadelphia, Pennsylvania 19137
Attn: ORDBA-1320

Office of Scientific Research
Department of the Air Force
Washington, D.C. 20333
Attn: Solid State Div. (SRPS)

Aerospace Research Labs
Wright-Patterson AFB
Building 450
Dayton, Ohio 45433

Air Force Materials Lab (LA)
Wright-Patterson AFB
Dayton, Ohio 45433

NASA Headquarters
Washington, D.C. 20546
Attn: Code RRM

NASA
Lewis Research Center
21000 Brookpark Road
Cleveland, Ohio 44135
Attn: Library

National Bureau of Standards
Washington, D.C. 20234
Attn: Metallurgy Division
Inorganic Materials Division

Atomic Energy Commission
Washington, D.C. 20545
Attn: Metals and Materials Branch

Defense Metals and Ceramics
Information Center
Battelle Memorial Institute
505 King Avenue
Columbus, Ohio 43201

Director
Ordnance Research Laboratory
P.O. Box 30
State College, Pennsylvania 16801

Director Applied Physics Lab.
University of Washington
1013 Northeast Fortieth Street
Seattle, Washington 98105

Metals and Ceramics Division
Oak Ridge National Laboratory
P.O. Box X
Oak Ridge, Tennessee 37830

Los Alamos Scientific Lab.
P.O. Box 1663
Los Alamos, New Mexico 87544
Attn: Report Librarian

Argonne National Laboratory
Metallurgy Division
P.O. Box 229
Lemont, Illinois 60439

Brookhaven National Laboratory
Technical Information Division
Upton, Long Island
New York 11973
Attn: Research Library

Library
Building 50, Room 134
Lawrence Radiation Laboratory
Berkeley, California

Professor G.S. Ansell
Rensselaer Polytechnic Institute
Dept. of Metallurgical Engineering
Troy, New York 12181

Professor H.K. Birnbaum
University of Illinois
Department of Metallurty
Urbana, Illinois 61801

Dr. E.M. Breinan
United Aircraft Corporation
United Aircraft Research Lab.
East Hartford, Connecticut 06108

Professor H.D. Brody
University of Pittsburgh
School of Engineering
Pittsburgh, Pennsylvania 15213

Professor J.B. Cohen
Northwestern University
Dept. of Material Sciences
Evanston, Illinois 60201

Professor M. Cohen
Massachusetts Institute of Technology
Department of Metallurgy
Cambridge, Massachusetts 02139

Professor B.C. Giessen
Northeastern University
Department of Chemistry
Boston, Massachusetts 02115

Dr. G.T. Hahn
Battelle Memorial Institute
Department of Metallurgy
505 King Avenue
Columbus, Ohio 43201

Professor R.W. Heckel
Carnegie-Mellon University
Schenley Part
Pittsburgh, Pennsylvania 15213

Dr. David G. Howden
Battelle Memorial Institute
Columbus Laboratories
505 King Avenue
Columbus, Ohio 43201

Professor C.E. Jackson
Ohio State University
Dept. of Welding Engineering
190 West 19th Avenue
Columbus, Ohio 43210

Professor G. Judd
Rensselaer Polytechnic Institute
Dept. of Materials Engineering
Troy, New York 12181

Dr. C.S. Kortovich
TRW, Inc.
23555 Euclid Avenue
Cleveland, Ohio 44117

Professor D.A. Koss
Michigan Technological University
College of Engineering
Houghton, Michigan 49931

Professor A. Lawley
Drexel University
Dept. of Metallurgical Engineering
Philadelphia, Pennsylvania 19104

Dr. H. Margolin
Polytechnic Institute of New York
333 Jay Street
Brooklyn, New York 11201

Professor K. Masabuchi
Massachusetts Institute of Technology
Department of Ocean Engineering
Cambridge, Massachusetts 02139

Dr. G.H. Meier
University of Pittsburgh
Dept. of Metallurgical and Materials
Engineering
Pittsburgh, Pennsylvania 15213

Professor J.W. Morris, Jr.
University of California
College of Engineering
Berkeley, California 94720

Professor K. Ono
University of California
Materials Department
Los Angeles, California 90024

Professor W.F. Savage
Rensselaer Polytechnic Institute
School of Engineering
Troy, New York 12181

Dr. C. Shaw
Rockwell International Corp.
P.O. Box 1085
1049 Camino Dos Rios
Thousand Oaks, California 91360

Professor O.D. Sherby
Stanford University
Materials Sciences Dept.
Stanford, California 94300

Professor J. Shyne
Stanford University
Materials Sciences Department
Stanford, California 94300

Dr. W.A. Spitzig
U.S. Steel Corporation
Research Laboratory
Monroeville, Pennsylvania 15146

Dr. E.A. Starke, Jr.
Georgia Institute of Technology
School of Chemical Engineering
Atlanta, Georgia 30332

Professor N.S. Stoloff
Rensselaer Polytechnic Institute
School of Engineering
Troy, New York 12181

Dr. E.R. Thompson
United Aircraft Research Lab.
400 Main Street
East Hartford, Connecticut 06108

Professor David Turnbull
Harvard University
Division of Engineering and Applied
Physics
Cambridge, Massachusetts 02139

Dr. F.W. Wang
Naval Ordnance Laboratory
Physics Laboratory
White Oak
Silver Spring, Maryland 20910

Dr. J.C. Williams
Rockwell International
Science Center
P.O. Box 1085
Thousand Oaks, California 91360

Professor H.G.F. Wilsdorf
University of Virginia
Department of Materials Science
Charlottesville, Virginia 22903

Dr. M.A. Wright
University of Tennessee
Space Institute
Dept. of Metallurgical Engineering
Tullahoma, Tennessee 37388